Polymer 345 (2026) 129604

Contents lists available at ScienceDirect

Polymer

journal homepage: www.elsevier.com/locate/polymer

Sorption and mass transport of water in polyimides: quantifying first- and second-shell and their dynamics

C. Brondi [a], A. Correa [b], G. Mensitieri [c,d], P. Musto [d], S. Scala [e,c], G. Scherillo [c,*], A. Baldanza [c,f,**]

[a] Department of Engineering and Science, Faculty of Technological and Innovation Sciences, Universitas Mercatorum, 00186, Rome, Italy
[b] Department of Chemical Science, University of Naples Federico II, 80126, Naples, Italy
[c] Department of Chemical, Materials and Industrial Production Engineering, University of Naples Federico II, 80125, Naples, Italy
[d] Institute for Polymers, Composites and Biomaterials, National Research Council of Italy, 80078, Pozzuoli (Naples), Italy
[e] Department of Neurosciences, Reproductive and Odontostomatological Sciences, University of Naples Federico II, 80125, Naples, Italy
[f] Scuola Superiore Meridionale, 80138, Naples, Italy

ARTICLE INFO

Keywords:
Glassy polyetherimide
Non-equilibrium PC-SAFT
Water sorption kinetics

ABSTRACT

Water sorption thermodynamics in glassy polymers is a salient issue in the context of accurately modeling membrane-based separation processes and tailoring the barrier properties of polymers for various technological applications. To this end, the water sorption thermodynamics of glassy polymers, two polyimides (6FDA-ODA and 6FDA-6FpDA), and a polyetherimide (Ultem®) have been interpreted within the framework of the Non-Equilibrium Thermodynamics Glassy Polymer-Perturbed Chain-Statistical Associating Fluid Theory (NETGP-PC-SAFT). This approach accounts for associative contributions, thereby enabling the quantitative reproduction of the complex interactional scenario exhibited by the three systems analyzed. This investigation also provided, for the first time, a validation of the NETGP-PC-SAFT model when self and cross-interactions occur in a polymer-penetrant system, by comparing model predictions with data from vibrational spectroscopy. Indeed, this theoretical approach enabled the quantitative estimation of the various types of sorbed water populations (i.e., water molecules that form the first and second hydration shells, respectively, related to water-polymer and water-water hydrogen bonding interactions) that successfully corresponded to the experimental outcomes. This interactional scenario has been further investigated through Density Functional Theory (DFT) calculations aimed at determining hydrogen-bonding energies and at confirming the involved interactive sites suggested by in situ Fourier-transform infrared spectroscopy. Following the validation of the NETGP-PC-SAFT model in terms of sorption thermodynamics, the model was implemented within the Standard Diffusion (SD) model to self-consistently describe water mass transport in the glassy PEI. This approach yielded a satisfactory data fit for the overall water sorption kinetics and concurrently predicted the time-evolution of the two distinct water populations with excellent concurrence to the experimental outcomes derived from in situ vibrational spectroscopy.

1. Introduction

The sorption of gases and vapors in polymers is of significant technological importance in a number of industrial sectors. For instance, this phenomenon is relevant in the context of membranes utilized for the separation of liquid and gas mixtures [1,2]. Additionally, it plays a crucial role in the field of barrier polymers employed in packaging applications [3,4]. Furthermore, the sorption of gases and vapors in polymers is pertinent to polymer composites [5]. A rigorous investigation into the sorption thermodynamics and kinetics of low-molecular-weight compounds (LMWC) in polymers is of significant practical and theoretical interest. This investigation draws upon a wide range of research methods, including experimental characterization techniques [6–10], theoretical approaches [11–13], and molecular simulations [14–16], as extensively documented in the existing literature.

Polyetherimide (PEI) and 4,4′-(hexafluoroisopropylidene)diphthalic anhydride (6FDA) - based polyimides are relevant materials for

* Corresponding author.
** Corresponding author.
E-mail addresses: gscheril@unina.it (G. Scherillo), antonio.baldanza@unina.it (A. Baldanza).

https://doi.org/10.1016/j.polymer.2026.129604
Received 13 November 2025; Received in revised form 5 January 2026; Accepted 13 January 2026
Available online 13 January 2026

membrane applications due to their permeability and selectivity properties and excellent resistance to organic solvents [17]. PEI is an amorphous thermoplastic polymer with a relatively high glass transition temperature (216 °C). Its aromatic groups confer high thermal resistance, and the presence of ether groups provides chain flexibility [18–20]. Applications of PEI range from gas separation [21,22] to polymer matrices with high thermal stability for nanocomposites in energy storage [23] and flexible electrothermal heaters [24]. Depending on the partial or total fluorination of the polymer backbone, 6FDA-based polyimides may display a wide range of molecular architectures [25] that significantly impact mechanical properties, gas permeability and selectivity, and resistance to organic solvents. These properties make these polymers the material of choice for membrane-based separations [26–28].

Understanding the molecular-level interactions between the polymer backbone and low-molecular-weight penetrants is crucial for the optimal design of separation processes. In particular, hydrogen-bonding (HB) interactions significantly impact membrane mass transport and, consequently, the performance of separations involving water and alcohols [29–33]. A thorough study of water mass transport and sorption thermodynamics is necessary for glassy polymer membranes exposed to humid gaseous streams [34,35]. At room temperature, polymers with a high glass transition temperature remain glassy even when exposed to a high-humidity environment. On the timescale of interest for common sorption and mass transport processes, the volume of the polymer-water mixture can be assumed to be "frozen" in the out-of-equilibrium state of the pure polymer. The macromolecular chains are "locked" into the initial configuration established right before sorption begins. Similarly, during the sorption process, the polymer mass density field is also the same as that of the pure polymer right before the sorption process begins. Assuming a spatially uniform polymer sample, the macroscopic mass density of the pure polymer is accessible through experimentation and is dictated by its previous thermomechanical history.

Based on these considerations, when a glassy polymer is exposed to a time-invariant water vapor phase, the water concentration inside the polymer attains an apparently constant value. However, this value differs from that corresponding to the "true" phase-equilibrium condition, which is only asymptotically reached after an infinite amount of time. This apparent phase equilibrium condition will be referred to as a "pseudo-equilibrium" condition here. Standard equilibrium sorption thermodynamics models cannot be used to address the related apparent penetrant solubility. To address pseudo-equilibrium sorption thermodynamics, the non-equilibrium thermodynamics glassy polymer (NETGP) approach has been proposed in the literature to extend equilibrium penetrant sorption thermodynamics models to the case of pseudo-equilibrium sorption in non-equilibrium glassy polymers [36,37].

In principle, this framework can be used to extend equilibrium thermodynamics models based on equation of state (EoS) approaches, among others. This approach uses thermodynamics with internal state variables and considers either the volume of the polymer phase or the polymer mass density as the sole internal state variable of the glassy mixture. Briefly, the polymer's mass density is not a function of the state variables, but rather an additional independent variable. Its value is determined by the polymer's thermo-mechanical history, rather than being calculated using the selected equilibrium EoS. This value can be retrieved from experimental measurements or empirical expressions. In particular, the NETGP procedure has been used to extend the Perturbed-Chain Statistical Associating Fluid Theory (PC-SAFT), successfully describing the sorption thermodynamics of gases and vapors in amorphous glassy polymers [38]. However, the analysis was limited to cases in which specific interactions can be neglected. Thus, the pure mean-field PC-SAFT model has been adopted, in which association terms are not considered. It has been proven that in pure "mean-field" EoS models (i.e., when only the action of dispersive forces is accounted for), phase pseudo-equilibrium between a glassy polymer phase and a gaseous/vapor mixture of penetrants is dictated by equating the equilibrium chemical potential (μ_i^{EQ}) in the gaseous/vapor phase and the non-equilibrium chemical potential (μ_i^{NE}) in the polymer/penetrant glassy phase for each penetrant i simultaneously. The latter is provided by the NETGP approach [36,37]. Notably, the same authors also demonstrated that μ_i^{NE} expressions can be obtained in NVT ensemble from the corresponding equilibrium expressions for the chemical potential of the penetrant within the polymer phase, as provided by an EoS-based model (e.g., the PC-SAFT model). In these models, the adopted polymer density value is not equilibrium-based, but rather the fixed, out-of-equilibrium density of the glassy polymer within the mixture.

Building on this latter result, Davis et al. [39] and Liu et al. [40] implemented the NETGP framework to extend, for the first time, a version of the PC-SAFT that included association terms, providing a satisfactory description of H_2O sorption in an amorphous, glassy PMMA membrane. However, it should be noted that extending the NETGP-PC-SAFT model would have required reexamining the entire NETGP procedure. Indeed, the NETGP extension procedure for EoS models, particularly the key results consisting of pseudo-equilibrium conditions for chemical potentials and the ability to calculate non-equilibrium chemical potentials using proper equilibrium expressions, has been theoretically validated for EoS models with only one internal state variable for the glassy phase (i.e., polymer mass density). The presence of association terms introduces an additional set of internal state variables, $\boldsymbol{x}$, representing the fraction of sites not involved in specific interactions for each association site type within the glassy phase [41,42]. This circumstance requires verification of the relevant assumptions adopted in the NETGP procedure.

Here, it is useful to recall the analysis that Michelsen performed on the theory developed by Chapman and Radosz [41] for association contribution, as presented in his seminal paper [42]. In particular, Michelsen clarified that the set of association equations introduced by Sadowsky et al. [43] within the PC-SAFT framework results from the minimization conditions of the Helmholtz energy in an NVT ensemble with respect to the set $\boldsymbol{x}$. These equations represent equilibrium conditions alongside the EoS, meaning this set of equations only holds at true equilibrium. In this respect, the procedure followed by Davis et al. [39] and Lui et al. [40] that utilizes this set of equations is implicitly based on the assumption of Instantaneous Equilibrium (IE) for the association contacts within the glassy phase. In other words, the set of internal state variables, $\boldsymbol{x}$, is imposed to satisfy the related minimization conditions for Helmholtz energy within the glassy mixture, evaluated in correspondence with the non-equilibrium polymer density [44]. However, this implicit assumption was neither explicitly stated nor verified in their implementation of the NETGP approach.

According to the IE assumption, the set $\boldsymbol{x}$ becomes a function of temperature, volume, and composition in the glassy phase. Based on this, in a recent paper [45], we proved that the original NETGP pseudo-equilibrium conditions still hold. However, a proper re-expression of μ_i^{NE} is necessary to apply these conditions. We also note that under the IE assumption, the penetrant μ_i^{NE} can be expressed as its equilibrium expression calculated with respect to the out-of-equilibrium polymer mass density. For readability, we summarized the fundamentals of this procedure in the Supporting Information (SI) file of our contribution and referred to the previous publication [45] for full details.

The IE assumption is rooted in the fact that the local dynamics of association contacts are much faster than the evolution dynamics of the other internal variable, the polymer density. This IE assumption has already been successfully implemented by applying the NETGP approach to the non-random hydrogen bonding (NRHB) model [35,44] for water-glassy polymer systems, as well as a to a PC-SAFT version that also accounts for possible penetrant-induced swelling of methanol-glassy polyimide mixtures [45].

One preliminary objective of this study is to evaluate the reliability of

the IE assumption employed in the NETGP procedure. This will be accomplished by comparing the qualitative and quantitative predictions of the theoretical model with the relevant outcomes obtained through in situ FT-IR spectroscopy and Molecular Dynamics (MD) simulations. The comparison will focus on the different types of specific interactions established within polymer-water systems. To this end, we have exploited a set of sorption data we collected in previous investigations for different glassy amorphous polymer/water systems, specifically 6FDA-ODA/H_2O, 6FDA-6FpDA/H_2O [46,47] and PEI/H_2O [48]. 6FDA-ODA and 6FDA-6FpDA are two fluorinated polyimides where 6FDA-ODA stands for [(hexahydrofluoroisopropylidene) diphthalic anhydride (6FDA), 4,4′-diaminodiphenyl ether (ODA)] and 6FDA-6FpDA stands for [(hexahydrofluoroisopropylidene) diphthalic anhydride (6FDA), 4,4′-(hexafluoroisopropylidene) dianiline (6FpDA)] while PEI is a polyetherimide (Poly([2,2′-bis(3,4-dicarboxyphenoxy) phenylpro pane]-2-phenylene-bisimide), commercially available under the tradename of Ultem® 1000. The molecular structures of the investigated polymers are reported in Scheme 1.

To further validate the results predicted by the NETGP-PC-SAFT, quantum chemical calculations were performed using Density Functional Theory (DFT) for the PEI/H_2O system. These calculations aimed to determine the bonding energy and confirm the specific sites involved in the interactions.

After validating the NETGP-PC-SAFT model in terms of sorption thermodynamics, this study focuses on extending it to address water sorption kinetics within a polymer-penetrant glassy phase. The study uses the PEI-water system as a case study.

In fact, mass transport has been modeled by exploiting the expressions for chemical potentials provided by the NETGP-PC-SAFT model under the IE assumption to calculate the driving force for the diffusive flux of the penetrant (see Section 3 for details). This approach is based on the Standard Diffusion (SD) model originally proposed by Minelli et al. [49,50]. To the best of our knowledge, only one attempt has been made in the literature to model mass transport in glassy polymer-penetrant phases by adopting the NETGP-PC-SAFT framework to express the driving force of the diffusion process in the presence of specific cross- and self-interactions. This was performed by Marshall et al. [51], who extended the NETGP-PC-SAFT approach by developing the Dry Glass Reference Perturbation Theory (DGRPT). This theory addresses penetrant-induced swelling in glassy polymer-penetrant phases and solvent pervaporation through glassy polymeric membranes. However, the DGRPT framework was only used to express the boundary conditions, whereas the constitutive equations for the diffusion process used classic phenomenological Stefan-Maxwell equations. Conversely, the original NETGP-PC-SAFT framework was implemented in Ref. [52] to self-consistently express the driving force for water diffusion in glassy polyvinylpyrrolidone-based polymers. For the first time, it was adopted a constitutive Stefan-Maxwell-inspired equation for the penetrant diffusion driving force. This equation differs from the SD model adopted in the present contribution [35,49,50,53–55].

Another significant aspect of the present investigation is the detailed analysis of the evolution kinetics of the two types of water molecules present in the PEI/H_2O system. In situ vibrational spectroscopy analysis revealed the presence of water molecules that interact with sites on PEI macromolecules via hydrogen bonding (known as 'first shell' water), as well as water molecules that interact via hydrogen bonding with 'first shell' water (forming 'second shell' water).

This experimental approach also enabled a quantitative assessment of the concentrations of the two types of water molecules at equilibrium and during the sorption process. In particular, the quantitative estimation of the evolution kinetics of water populations required an analysis that is presented here for the first time in the literature (see Section 4.2.1). Predictions of the kinetic evolution of the two types of water molecules, obtained by applying the SD model in combination with the NETGP-PC-SAFT approach (NETGP-PC-SAFT-SD model) under the illustrated IE assumption for specific interactions (associations), were in perfect agreement with the experimental data. This result further supports the suitability of the IE assumption for glassy systems with specific interactions. The NETGP-PC-SAFT-SD model is general and can be applied to the sorption kinetics of water (and other interacting penetrants) in any glassy polymer well below its glass transition temperature, provided the relevant model parameters can be obtained, for instance, by following the procedure proposed in the present investigation.

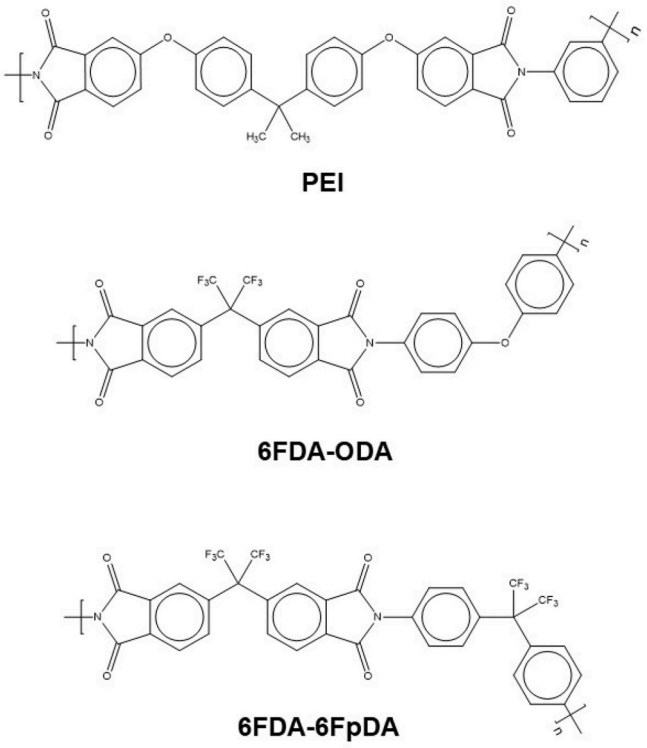

Scheme 1. Molecular structures of investigated polymers.

2. Materials and methods

2.1. Materials

Poly([2,2′-bis(3,4-dicarboxyphenoxy) phenylpropane]-2-phenylene-bisimide), commercially available under the tradename of *Ultem® 1000,* was kindly supplied by *General Electric*. It had $\overline{M}_w = 3.0 \times 10^4 Da$, $\overline{M}_n = 1.2 \times 10^4 Da$ (GPC), $T_g = 210\ ^\circ C$ (DSC) and density = 1.267 g/cm^3 (as determined by flotation). Water Milli-Q grade for sorption experiments was degassed through at least five freezing-thawing cycles.

Freestanding films of *Ultem®* 1000 were prepared by casting a 5 wt % solution of the polyetherimide in chloroform. The nascent film was first dried at atmospheric conditions for 2 days and then in a vacuum oven at 120 °C for 48h, to remove residual traces of solvent. The thickness of the film produced with this protocol was 40 ± 1 μm.

2.2. FT-IR sorption experiments

Time-resolved spectra were collected in the transmission mode. The polymer film, accommodated in a vacuum-tight FT-IR sorption cell, was exposed to water vapor at constant temperature (30 °C) and different pressures of water vapor. The sorption cell, equilibrated with recirculating water to ±0.1 °C, was connected through service lines to a liquid water reservoir, a turbo-molecular vacuum pump and a MKS Baratron 121 pressure transducer (Andover, MA, full scale 100 Torr, resolution 0.01 Torr, accuracy ±0.5 % of the reading). Before sorption the polymer film was dried *in-situ* overnight under vacuum at the experimental

temperature to eliminate moisture sorbed from the environment. Differential sorption tests were performed by increasing stepwise the relative pressures of water vapor within the range 0–0.6. The kinetic analysis was made on an integral sorption test at $P/P_0 = 0.6$. The spectroscopic measurements were performed by a Spectrum GX interferometer from Perkin-Elmer (Norwalk, CT), equipped with a Ge/KBr beam splitter and a wide-band DTGS detector. Collection parameters were set as follows: resolution = 4 cm^{-1}; Optical Path Difference (OPD) velocity = 0.5 cm/s; spectral range 4000–600 cm^{-1}. A single data collection per spectrum was made, which took 2.0 s to complete under the selected instrumental conditions. Spectra were acquired in the single-beam mode using a dedicated software package for *time-resolved* spectroscopy (*Timebase*, Perkin-Elmer).

Full absorbance spectra (i.e., polymer plus absorbed water) were obtained using as background spectrum the cell without the sample under the test conditions. The spectra representative of absorbed water were obtained by difference spectroscopy, i.e. by subtracting from the full absorbance spectrum as defined above, the spectrum of the dry sample.

3. Theoretical background

3.1. NETGP-PC-SAFT

Perturbed-Chain Statistical Association Fluid Theory (PC-SAFT) is an EoS model for multicomponent fluid systems [56], in which each molecule is schematized as a chain of equivalent spherical segments and the reduced Helmholtz energy is obtained by a perturbation procedure, in which the reference fluid is made by hard spherical segment chains [43]. Specifically, the reduced Helmholtz energy of a generic fluid phase, denoted by $\tilde{a}$, is derived as the sum of distinct contributions, accounting for both possible association interactions and/or dipolar interactions, in addition to the "mean field" interactions:

$$\tilde{a} = \frac{A}{NkT} = \tilde{a}^{id} + \tilde{a}^{hc} + \tilde{a}^{disp} + \tilde{a}^{assoc} + \tilde{a}^{dp} \tag{1}$$

where N, K and T represent the total number of molecules, the Boltzmann constant and the temperature, while $\tilde{a}^{id}$, $\tilde{a}^{hc}$, $\tilde{a}^{disp}$, $\tilde{a}^{assoc}$ and $\tilde{a}^{dp}$ indicate, respectively, the ideal gas, the hard sphere chain reference, the dispersion, the associative and dipolar contributions to $\tilde{a}$. The PC-SAFT model, then, is able to account for a series of possible interactions such as Lewis Acid – Lewis Base, Hydrogen Bonding and dipolar interactions. Each species i is characterized by three pure "mean-field" component parameters: the segment diameter at $T = 0$ K, σ_i, the number of segments m_i, and the depth of the potential well, $\frac{\varepsilon_i}{k}$. In the case of multicomponent systems, the "mean-field" parameters can be retrieved by applying the following pairwise mixing rules:

$$\sigma_{ij} = \frac{\sigma_i + \sigma_j}{2} \tag{2}$$

$$\varepsilon_{ij} = \sqrt{\varepsilon_i \varepsilon_j}\,(1 - k_{ij}) \tag{3}$$

where i and j stand for two of the components that form the mixture, k_{ij} represents the corresponding "mean-field" dimensionless binary interaction parameter introduced for any couple i - j and is used as an adjustable parameter, whose value is generally close to zero.

The associative type of contribution introduced in the PC-SAFT model was previously developed by Chapman [41] and it is introduced for each kind of specific interaction established between an associative site of kind A on molecules i, A_i, and an associative site of kind B on molecules of species j, B_j. Under this formulation, two associated pairwise parameters are required, i.e., $\varepsilon^{A_iB_j}$ and $k^{A_iB_j}$, being respectively the specific association energy and the so-called association volume. It is important to note that this scheme operates under the assumption that each distinct associative site is univocally associated with a particular species within the system under consideration. In turn, each species may exhibit one or more distinct typologies of associative sites. The physics of the system under study dictates that only dual associative sites (i.e., proton donor/proton acceptor or Lewis acid/base) can establish specific interactions. In principle, the association parameters can be regarded as adjustable and can be estimated by a non-linear regression of equilibrium data of fluid mixtures involving the corresponding specific interactions. In particular, for self-associative interactions occurring between sites both belonging to a pure component (i=j), the related couple of association parameters can be determined along with the three pure "mean-field" parameters by a non-linear regression of liquid-vapor (LV) phase equilibrium data in the case of low molecular weight compounds, or of equilibrium dilatometric data for polymeric species.

In the case of cross-interactions ($i \neq j$), the value of the corresponding cross-association parameters, to minimize the number of adjustable parameters, can be estimated according to the following mixing rules [57,58]:

$$\varepsilon^{A_iB_j} = \frac{1}{2}\left(\varepsilon^{A_iB_i} + \varepsilon^{A_jB_j}\right) \tag{4}$$

$$k^{A_iB_j} = \sqrt{k^{A_iB_i}\,k^{A_jB_j}}\left(\frac{\sqrt{\sigma_i\sigma_j}}{1/2(\sigma_i + \sigma_j)}\right)^3 \tag{5}$$

The mixing rules proposed in Ref. [57] are particularly well-suited to address the case of two self-associating species, in which each species displays one typology of association site of kind A and one of kind B. An extension of these mixing rules to the case in which one of the two species is non-self-associating was proposed by Ref. [58], who introduced a fictive self-association (to be used exclusively in the implementation of the mixing rules) for the association site of interest on the non-self-association species. In this regard, for systems exhibiting a sufficient number of distinct cross-interactions and/or the presence of non-self-associating sites, it may be more appropriate to ascertain these cross-association parameters through regression analysis of a particular dataset of binary systems. The strategy employed in the present contribution to estimate both the self- and the cross-interaction parameters is addressed in the results section.

Finally, the dipolar contribution introduces a set of additional parameters associated with each kind of dipole present in the system. Dipolar moments can be estimated through ab initio calculation or by treating them as additional adjustable parameters to be retrieved, along with the association and "mean field" ones, from LV phase equilibrium data of pure components. With regard to the systems under consideration in the present contribution, the interactive scenario delineated by the FT-IR and DFT investigations suggests that strong specific interactions (e.g., HB) predominate, thereby justifying the neglect of the dipolar contribution. Consequently, the formulation of the NETGP-PC-SAFT model considers solely the contribution of "mean-field" and associative terms.

As discussed in Section 1 and elaborated in the SI file, the NETGP-PC-SAFT model, incorporating the association term (under the IE assumption), dictates that the pseudo-equilibrium of phase is attained by equating the equilibrium chemical potential of each penetrant evaluated in the external phase, μ_i^{EQ}, with the appropriate expression of non-equilibrium chemical potential that accounts for the IE assumption within the glassy polymer-penetrant phase, μ_i^{IE}.

The expression of μ_i^{EQ} is obtained, in the NPT ensemble, by coupling the corresponding general non-equilibrium expression of the chemical potential and the minimization conditions of the Gibbs energy towards the phase volume as well as the set of associative internal state variables. Conversely, the expression of μ_i^{IE} is obtained by coupling the corresponding general non-equilibrium expression (i.e. the general one provided by PC-SAFT model with association term, before implementing any minimization condition) only with the minimization conditions

towards the set of association variables (evaluated at the out-of-equilibrium value of the polymer mass density within the glassy mixture). On this basis, the complete set of equations necessary for the calculation of penetrant pseudo-equilibrium phase conditions is entirely provided by expressions derived from the PC-SAFT model endowed with association contribution (see SI for comprehensive details). In particular, the minimization conditions towards the set of the associative internal state variables are given by Ref. [41]:

$$x^{A_i} = \left(1 + \sum_j \frac{\rho_j}{Mw_j} \sum_{B_j} x^{B_j} \Delta^{A_i B_j}\right)^{-1} \tag{6}$$

Hereafter, $\Delta^{A_i B_j}$ indicates the molecular association strength for the interaction $A_i B_j$, which is function of the two corresponding associative parameters, ρ_j stands for the *j-th* component mass density and x^{A_i} represents the fraction (as referred to its total amount) of association sites of kind *A* on the *i-th* species that are not involved in any possible association interaction and Mw_j is the molecular mass of *j-th* component.

The general non-equilibrium expression for the chemical potential is provided by the sum of the ideal, hard-chain, dispersion and associative contributions. Regarding the associative contribution, we have adopted the approach of [42] (see also the SI file), while for the first three terms the reader is referred to the original literature [43]. To summarize, the general non-equilibrium expression for the association contribution, coupled with equation (6), provides the following expression for the IE penetrant chemical potential within the glassy polymeric phase:

$$\frac{\mu_i^{IE,assoc}}{RT} = \sum_{A_i} (log\ x^{A_i}) - \frac{1}{2} \sum_k \sum_j \frac{\rho_k}{Mw_k} \frac{\rho_j}{Mw_j} \sum_{A_k} \sum_{B_j} x^{A_k} x^{B_j} Mw_i \frac{\partial \Delta^{A_k B_j}}{\partial \rho_i} \tag{7}$$

where the superscript IE, as discussed, refers to the underlying assumption of instantaneous equilibrium for the associative term. We remark here that: a) eq. (7) is obtained starting from the most general non-equilibrium expression of the *i-th* molar chemical potential, recognizing that some terms in such general expression are null under the IE assumption according to eq. (6), and b) the set of internal state variables *x* appearing in eq. (7) is intended to be calculated using eq. (6) in correspondence of the fixed out-of-equilibrium polymer mass density. Finally, the operative expression of μ_i^{EQ} is determined by coupling equations (6) and (7) with also the EoS properly calculated at the given *T* and *P* and external phase composition. The EoS expression can be calculated as the sum of the ideal, hard-chain and dispersion terms developed in original literature of PC-SAFT by group of Sadowski [43] and the associative contribution proposed by Ref. [42].

3.2. Diffusion model based upon NETGP-PC-SAFT

In this section we briefly discuss the implementation of the NETGP-PC-SAFT framework into the 'Standard Diffusion' (SD) model of mass transport of low molecular weight compounds (LMWCs) in glassy amorphous polymers (hereafter, referred to as NETGP-PC-SAFT-SD model). The SD approach has been originally proposed and extensively validated by Doghieri et al. [49,50,53] in combination with the NETGP framework based on the Sanchez and Lacombe EoS lattice fluid model (SL) [36,37,59] (referred to as NETGP-SL-SD model or NELF-SD) to express the driving force for the diffusive flux of a penetrant in a glassy polymer for binary and ternary steady-state permeation processes. Since the SL EoS model accounts only for dispersive (mean field') interactions, the NETGP-SL-SD, can cope only with systems that do not display specific interactions. Later, to account for possible occurrence of strong specific interactions, this same framework was adopted but based upon the thermodynamic consistent Non-Random Hydrogen Bonding (NRHB) EoS theory [60,61] (NETGP-NRHB-SD model) [35,55] instead of the SL EoS theory, to deal with mass transport of gas/water vapor binary mixtures in glassy polymers. To this aim, a proper expression for the penetrant mobility coefficient was also proposed which we use in the present contribution within the NETGP-PC-SAFT-SD model. For full details regarding the SD approach, we refer the reader to the original literature [50,55]. In the following we only report a short description of such an approach, focused on binary polymer-penetrant systems displaying cross and self-specific interactions.

In the SD approach, the driving force for the mass diffusive flux of the penetrant within the glassy phase is provided by the gradient of μ_i^{IE}, whose expression is the same implemented to model sorption thermodynamics. In accordance with the extant literature, the SD constitutive equations for diffusive fluxes have been developed in the limit of low mass concentration of the penetrants. This assumption is reasonable in the experimental conditions of interest. Based on the principles of linear irreversible thermodynamics [62], the SD model posits the following constitutive equations for the diffusion process in a binary polymer-penetrant glassy mixture, under the assumption of uniform temperature and pressure fields, denoted by *T* and *P*, respectively (neglecting the effect of gravitational forces and considering exclusively non-ionic species) [50]:

$$\boldsymbol{J_1} = L_{11}\boldsymbol{d_1} + L_{1p}\boldsymbol{d_p} \tag{8.a}$$

$$\boldsymbol{J_p} = L_{p1}\boldsymbol{d_1} + L_{pp}\boldsymbol{d_p} \tag{8.b}$$

where subscripts 1 and *p* represent, respectively, the LMWC (i.e., the penetrant) and the polymer. $\boldsymbol{J_i}$ represents the diffusive mass flux of *i*-th component with respect to the mixture mass average velocity, L_{ij} are 'mobility' scalar valued (positive) coefficients intrinsically defined by the constitutive equation (8), and finally $\boldsymbol{d_i}$, indicates the driving force contribution of the *i*-th component, which is in turn related to the corresponding gradient of molar chemical potential as defined by the following constitutive equation:

$$\boldsymbol{d_i} = -c_i \nabla \left(\frac{\mu_i^{IE}}{RT}\right)_{T,P} \tag{9}$$

where c_i represents the molar density of the *i*-th component and *R* the universal gas constant. Note that spatial vector field symbols are reported in bold except for the one obtained by operating the spatial gradient operator. According to the Gibbs-Duhem equation, the following restriction holds at any point of the mixture domain (that is here considered to be time invariant) at any instant of time, for the two driving forces [55,62]:

$$\boldsymbol{d_1} + \boldsymbol{d_p} = \boldsymbol{0} \tag{10}$$

In section S.2 of SI file, it is illustrated how the use of Gibbs-Duhem equation is legitimate in the case at hand of an out-of-equilibrium glassy polymer, under the IE assumption.

Inserting eq. (10) into eq. (8), one then obtains:

$$\boldsymbol{J_1} = \left(L_{11} - L_{1p}\right)\boldsymbol{d_1} \tag{11.a}$$

$$\boldsymbol{J_p} = \left(L_{p1} - L_{pp}\right)\boldsymbol{d_1} \tag{11.b}$$

In diluted conditions, the mutual cross mobility coefficients are assumed to be negligible with respect to the corresponding self-mobility ones ($L_{1p} \ll L_{11}$ and $L_{p1} \ll L_{pp}$). Finally, equation (11) become:

$$\boldsymbol{J_1} = L_{11}\,\boldsymbol{d_1} \tag{12.a}$$

$$\boldsymbol{J_p} = -L_{pp}\,\boldsymbol{d_1} = L_{pp}\,\boldsymbol{d_p} \tag{12.b}$$

Since, $\boldsymbol{J_1} + \boldsymbol{J_p} = \boldsymbol{0}$ (everywhere, at any instant of time) [62], it then results that $L_{11} = L_{pp}$. In fact, L_{ij} are generally function of concentration and *T* and in principle it is possible to have a process in which in a point at a given instant of time t, an arbitrary concentration set and temperature hold in correspondence of a $\boldsymbol{d_1} \neq \boldsymbol{0}$.

According to free-volume theories [63,64], the mobility coefficients

can be assumed to be a function of the local values of temperature T, penetrant mass fraction concentration ω_1, and fractional free volume (*FFV*), respectively, which is turn T and concentration dependent. On this basis, we have used the following expression for the sole mobility coefficient $L_{11} = L_{pp}$:

$$L_{11} = L_{1,0}\, exp\left(\frac{-E_{a,1}\,(1-\beta_1\omega_1)}{RT}\right) exp\left(-\frac{\gamma_1}{FFV}\right) \tag{13}$$

This equation has already been proposed and successfully implemented to model the concurrent steady-state mass transport of CO_2 and H_2O in glassy PEI [35]. Coefficients $L_{1,0}$ and $E_{a,1}$ (both assumed to be intrinsically positive) indicate, respectively, a constant pre-exponential factor of the penetrant and the activation energy for the elementary diffusive jump of the penetrant evaluated in the limit of its vanishingly small concentrations. Finally, γ_1 represents a phenomenological coefficient "weighting" the effect on the mobility coefficient of the 1/FFV term. The parameter β_1 is here introduced so that $\beta_1\omega_1$ represents a phenomenological term accounting for a concentration dependence of the penetrant activation energy. According to the physics of H_2O transport in PEI, as discussed afterwards, it is expected that the water activation energy decreases with its concentration so that the $\beta_1 > 0$. $L_{1,0}$, $E_{a,1}$ and β_1 can be assumed as adjustable parameters to be determined by a non-linear regression of sorption kinetics data, collected at different temperatures and different boundary and/or initial conditions. In the present investigation, the set of sorption kinetics data is referred only to one temperature so that the three parameters cannot be determined separately. In fact, the couple of parameters $L_{1,0}$, and $E_{a,1}$ as well as the couple of parameters $E_{a,1}$ and β_1 act as lumped parameters in the fitting procedure, that then considers only three adjustable parameters, i.e., γ_1, $L^*_{1,0}$ and β^*_1 (see eq. 14a,b), expected to be positive:

$$L^*_{1,0} = L_{1,0}\, \exp\left(-\frac{E_a}{RT}\right) \tag{14.a}$$

$$\beta^*_1 = \beta_1 \frac{E_a}{RT} \tag{14.b}$$

The concentration-dependent activation energy in eq. (13), associated to a diffusive elementary jump, is related to polymer-penetrant and, at higher penetrant concentration, to penetrant-penetrant specific interaction energies. The free volume term ($\frac{\gamma_1}{FFV}$) accounts, instead, for the volume available to local rearrangements of the polymeric chains needed to promote the formation of a cavity of suitable size and shape so that the penetrant elementary jump can occur.

Previous studies [48,65], have shown that two different water 'states' are present within the binary PEI/H_2O glassy phase, at the temperature and water activity values of interest here. The first state corresponds to a 'first shell' made of the H_2O molecules involved in cross-HB interactions occurring between a hydrogen atom of a H_2O molecule (acting as a proton donor, PD) and the oxygen of the carbonyl group (acting as a proton acceptor, PA) present along the polymer backbone. More in detail, in situ FT-IR quantitative analysis, MD simulations, and NETGP-NRHB model predictions, independently, point out that each 'first shell' molecule establishes simultaneously two cross-HB interactions bridging two polymer carbonyl groups; in particular, MD outcomes evidence a negligible interchain bridging with a preferential occurrence of intrachain bridging between the carbonyl groups located on two immediately contiguous imide groups along the PEI chain [48]. The second state consists of H_2O molecules establishing self-HB interactions with the oxygen (that acts as PA) of 'first shell' H_2O molecules, thus forming a 'second shell'.

In light of the aforementioned physical scenario, it can be deduced that the molecular water mass transport process encompasses the mobility of three distinct entities: 'first-shell' H_2O molecules, 'second shell' H_2O molecules and 'first shell/second shell' H_2O dimers. According to energetic and steric considerations, the "second shell" H_2O molecules are expected to exhibit the highest mobility and, since their relative concentration increases with the total water concentration within the mixture [48], it is reasonable to expect a decrease in the total average activation energy for water diffusion as a function of overall water concentration. This result should be phenomenologically accounted for by the $\beta_1\omega_1$ term in eq. (13), with $\beta_1 > 0$ and hence by a positive value of the corresponding lumped parameter, $E_{a,1}\beta_1$. Note that the increase of overall water concentration determines also an increase of the relative concentration of 'first-shell/second-shell' water dimers, whose mobility is expected to be lower also compared to the 'first shell' populations. However, energetic and, above all, steric considerations suggest that the relative contribution to the overall observed water transport mechanism of such dimeric entities is negligible, at least within the low/moderate water concentration range investigated, so that the prominent effect of the overall water concentration is likely associated to the relative increase of the more mobile 'second shell' molecules. Indeed, the values of the adjustable parameters obtained by the non-linear regressions of kinetics data are consistent with such physical picture, with a positive value of β^*_1 (see Table 3).

The last factor in eq. (13) accounts for the contribution of local fractional free volume (*FFV*), that represents the ratio of the local free volume to the total volume δV associated to an elementary region surrounding the current penetrant position. According to the free volume theory, the term in eq. (13) associated to *FFV* accounts for the local probability that an elementary diffusive jump of a penetrant molecule occurs. Indeed, for a given interactional scenario, such probability is expected to increase as a function of *FFV* thus determining a positive value of the parameter γ_1.

Assuming that the system is locally uniform within the elementary volume δV, a self-consistent estimate of *FFV* can be proposed based on the PC-SAFT theory [56,66]:

$$FFV \equiv \frac{(\delta V - \delta V^*)}{\delta V} = \frac{(\delta V - \delta V_{occ}/\eta)}{\delta V} = 1 - \frac{1}{\delta V}\frac{\pi}{6\eta}\sum_i n_{i,mol}\, m_i\, d_i^3 = 1 - \frac{\pi}{6\eta_{cp}}\sum_i \rho_{i,mol}\, m_i\, d_i^3 \tag{15}$$

where the summation is over the total number, n_t, of components present in the considered phase ($n_t = 2$ in the binary case of interest here). In eq. (15), δV_{occ} represents the total local volume occupied by the molecules of all components as provided by PC-SAFT while δV^* ($= \delta V_{occ}/\eta$) represents an 'effective' value of the occupied volume which includes also the interstitial volume, that is considered not to be available for a diffusive jump. $n_{i,mol}$ represents the number of molecules of species i present within the volume δV and d_i represents the segment diameter of the i-th component at the given temperature T (it can be calculated from σ_i, using PC-SAFT theory [56,66]). Finally, $\rho_{i,mol} = \rho_i/Mw_i$ is the local molecular number density of i-the component.

Eq. (15) is based on the fact that "interstitial" volume pockets confined among chains are less or not effective for an elementary diffusive jump to occur. To account for that, an 'effective' occupied volume, δV^*, is introduced which is higher than the 'true' occupied volume, δV_{occ}, by an average scaling factor, $1/\eta$. The latter has been estimated as being the highest possible value of the packing fraction of spherical segments that is equal to $\frac{\pi}{3\sqrt{2}}$. This phenomenological "correction" does not introduce any additional optimization parameter, and it is implicitly rooted on the assumption that the hard spheres arrangement locally reflects a lattice close-packed order.

Since eq. (15) just involves intensive quantities as well as molecular parameters of pure components, one can invoke the principle of local action, so that eq. (15) can be used to obtain the local expression of the fractional occupied volume. Note that the pure-component parameters sets are not function of the position and time in the case of isothermal process as is the one considered in the present investigation.

A similar approach for the estimation of the *FFV* has been

implemented by Sadowsky et al. [52] in modelling diffusion of H_2O in both glassy and rubbery polymer-penetrant phases. For the binary systems considered here, with a fixed value of $\rho_{p,mol}$, eq. (15) predicts, as expected, that the *FFV* decreases with increasing the water concentration. Indeed, such results is associated to the assumption that the penetrant does not introduce any swelling of the glassy matrix so that each local control volume associated to a fixed mass of the polymer is fixed.

The intrinsically positive coefficient γ_i introduced in eq. (13) accounts for the sensitivity of the mobility of the *i*-th penetrant to the available fractional free volume. It is then expected that γ_i increases as a function of the size of the molecule *i*, i.e., of its van der Waals volume. Since the shape of a penetrant molecule is generally not spherical, the probability of occurrence of an elementary diffusive jump depends, in a complex fashion, on both the relative size and the relative shape of the penetrant molecules with respect to the local geometry (shape and size) of the free volume, making the kinetic diameter of the *i*-th penetrant a more suitable parameter to be related to γ_i [67]. In addition, in the case of different populations of the penetrant *i*, such coefficient should be taken as a phenomenological average value, reflecting the varying size/shape of the different jumping units (i.e., in the case investigated here, the two types of monomers and the dimers).

A suitable expression for the penetrant diffusive flux as per eq. (12.a) along with eqs. (13) and (15) is then available and it is possible to model the sorption kinetics process of water in PEI based on the mass balance equation for the penetrant in the binary system of interest. We preliminarily observe that, according to equation (12), the polymer diffusive mass flux displays the same order of magnitude of that of the penetrant but, since the polymer mass density under dilute condition is much higher than that of the penetrant, the mass average velocity is very close to the polymer velocity. The latter is in turn assumed here, for any practical purpose, to be equal to the null vector in the lab fixed-frame of reference, on the basis of no-swelling assumption. Therefore, the penetrant mass diffusive flux $\boldsymbol{J_1}$ provided by eq. (12.a) represents also the overall mass flux of the penetrant within the adopted lab fixed-frame of reference.

Considering the case of a plane sheet of polymer, with a uniform thickness that is much smaller than the other two main dimensions, exposed to a uniform penetrant fluid phase, the transport process can be assumed one-dimensional along the thickness direction. In this case, the differential mass balance equation and the B.Cs. and I.Cs., are as follows:

$$\frac{\partial \rho_1}{\partial t} = -\frac{\partial J_1}{\partial z} \quad 0 < z < \xi, 0 < t < +\infty \tag{16.a}$$

$$\text{I.C.} \quad \rho_1(z, t=0) = \rho_1^{in} \quad 0 \le z \le \xi \tag{16.b}$$

$$\text{B.C.} \quad \rho_1(z=\{0,\xi\}, t) = \rho_1^{PE} \quad 0 < t < +\infty \tag{16.c}$$

where the superscript *in* indicates the initial condition, J_1 refers to the component of $\boldsymbol{J_1}$ along the thickness direction and the sample thickness is indicated as ξ. By expressing the penetrant diffusive mass flux according to eqs. 9 and (12).a, 13 and 15), eq. (16) define a one-dimensional non-linear PDE transient problem where the only unknown function is the time-dependent profile of the penetrant mass concentration $\rho_1(z,t)$, since the out-of-equilibrium mass polymer density field is assigned.

The chemical potential expressions which appear in the diffusion model proposed here are provided by the NETGP-PC-SAFT, under the IE assumption. To this regard, the "IE" penetrant chemical potential, in the binary case considered here, according to the discussion reported in the SI file, displays the following formal functional dependence:

$$\mu_1^{IE}(T, \rho_1, \rho_p) \equiv \mu_1^{NE}(T, \rho_1, \rho_p, \boldsymbol{x}^{IE}(T, \rho_1, \rho_p))$$

so that the penetrant mass diffusive flux, after application of derivative chain rules (under the assumption of uniform polymer mass density), is provided, in the one-dimensional case, by:

$$J_1 = \rho_1 L_{11} \left(\frac{\partial}{\partial \rho_1} \left(\frac{\mu_1^{IE}}{RT} \right) \frac{\partial \rho_1}{\partial z} \right) \tag{17}$$

The B.Cs. are obtained by assuming that at the external surface of the sample the solubility is dictated by imposing, at each instant of time, the pseudo-equilibrium condition (consistently provided by NETGP-PC-SAFT) between the polymeric phase and the external fluid phase.

We remark that the present approach, still based upon the local feature of association interactions, assumes the IE conditions at any given time and at any spatial point of the glassy mixture. This is a reasonable hypothesis since the association dynamics is expected to be much faster than the sorption penetrant concentration profile evolution.

Operatively we have solved the PDE problems provided by eqs. 16 and 17 with proper BCs, by using a finite discrete approach based on the method of lines [68] implemented in Matlab® R 2024. In particular, at any time integration step, adopting IE assumption, one solves eq. (6) in correspondence of the actual penetrant concentration values at the spatial nodes of the spatial discretization grid, so that the spatial derivatives in eqs. 16 and 17 can be calculated. The details of the procedure adopted to calculate all the derivatives involved in eq. (16) are reported in the Supporting Information file, whereas the spatial derivative in eq. (17) has been obtained numerically.

3.3. Quantum chemistry computational details and models

Quantum chemical calculations were performed using the DFT by the Gaussian09 package [69] at B3LYP level of theory [70–73]. Electronic configuration of all atoms was described by the 6–311++G** basis set [74–77]. If not indicated otherwise, all interaction energies, E_{coord}, herein reported were calculated as differences between the product energy and the reactants total energy, and all interaction energies were corrected for basis set superposition error (BSSE correction) with the counterpoise approach of Boys and Bernardi [48,65,78]. Negative values for E_{coord} mean stable PEI/H_2O adducts. All geometries reported in this paper were fully optimized. Vibrational analysis shows no imaginary frequencies for all reported minima. The PEI molecular model consists of a section of a single PEI monomeric unit (see Scheme S1, in SI file); such model has been successful adopted in previous studies [79]. In order to look at all possible interaction sites between water and PEI, several starting geometries have been tested.

4. Results and discussion

4.1. Sorption thermodynamics

4.1.1. Pure components parameters

The pure component parameters of the PC-SAFT model for water were obtained by simultaneously fitting liquid-vapor (LV) equilibrium data (e.g., saturation pressure, P_{sat}) and the corresponding equilibrium mass densities of the liquid (ρ_L) and vapor (ρ_G) phases.

Since water is a self-associating species, five parameters must be obtained from the fitting of experimental data: the three "mean-field" parameters (σ_1, ε_1 and m_1) and the two self-associating parameters ($\varepsilon^{A_1B_1}$ and $k^{A_1B_1}$), as described in the Theoretical Background section [43,66]. Hereafter, the subscript 1 refers to water. Cameretti et al. [80] observed that a satisfactory correlation of a set of pure water LV equilibrium data over a wide temperature range requires a phenomenological dependence of σ_1 on temperature according to the following equation:

$$\sigma_1(T) = \sigma_{1,0} + T_{d,1} \exp\left(T_{d,2}\, T\right) + T_{d,3} \exp\left(T_{d,4}\, T\right) \tag{18}$$

where $\sigma_{1,0}$, $T_{d,1}$, $T_{d,2}$, $T_{d,3}$, and $T_{d,4}$ is a set of adjustable parameters needed to determine σ_1 as a function of the temperature. In the present contribution we have adopted eq. (18) so that the adjustable parameters

for the case of water are provided by such set of parameters along with ε_1, m_1, $\varepsilon^{A_1B_1}$ and $k^{A_1B_1}$. The values obtained for water parameters are reported in Table 1. They are slightly different from those available in literature for the same set of adjustable parameters [80] since such previous studies did not include saturation vapor densities in the regression procedure. Within this framework, the association Scheme 2/2 (e.g. $N^{A_1} = 2$ and $N^{B_1} = 2$) has been used to represent the water self-interaction, with two equivalent proton acceptor sites (on the oxygen) and two equivalent proton donor sites (on the hydrogen), for each water molecule. The fitting procedure, applied to experimental data taken from Ref. [81], provided quite satisfactory results in the entire range of temperatures investigated, as reported in Fig. 1.

The pure component (PC) PC-SAFT parameters for the three polymers under investigation were obtained by simultaneously fitting equilibrium dilatometric data (ρ_L) for each compound [46,47]. Previous studies on the molecular structure and FT-IR investigations [46,47] suggest that all polymers exhibit a single type of associating site consisting of proton acceptor groups from the four carbonyls (C═O) in each repeating unit (i.e., $N^{A_p} = 8$, with two equivalent proton acceptors per carbonyl; subscript p refers to the polymer species). Since no proton donors are present along the chains, polymer self-association interactions have been neglected, and only the three "mean field" parameters need to be determined by the nonlinear regression procedure. Fig. 2 shows the results of fitting experimental data for the three polyimides with the PC-SAFT model. The model exhibits excellent fitting capability across the entire temperature and pressure range for all the polymers considered.

Table 1 shows the optimized "mean-field" and self-association parameter values for each polymer. Additionally, the table shows the number of each type of equivalent association site present on each polymer and water molecule (see columns 7 and 8).

It is worth noting that we adopted the procedure developed by Marshall and Bokis [82] for non-self-associating species to reduce the number of adjustable parameters to be determined for the polymer/-water cross-association interactions. In particular, for a carbonyl group on an i-th ketone molecule, Marshall et al. used the 2/0 association scheme (i.e., $N^{A_i} = 2$ and $N^{B_i} = 0$) and estimated the fictive self-association parameters $\varepsilon^{A_iB_i}$ and $k^{A_iB_i}$ for use in equations (4) and (5) to calculate the cross-interaction parameters with a series of suitable species. These fictive parameters were adopted as the only adjustable parameters to simultaneously fit the LV equilibrium data of several binary ketone-alcohol systems (since the self-interaction parameters of the OH groups in the alcohols were available in the literature). Based on a hydrogen bonding local feature, we assumed that the fictive self-associating parameters, $\varepsilon^{A_iB_i}$ and $k^{A_iB_i}$, of the C═O groups of the three polymers were equal to those of the C═O group of ketones, as determined by Marshall et al. [82]. Such values are reported in Table 1 (see columns 5 and 6). The "fictive" self-association parameters of the carbonyl groups are used in equations (4) and (5) to calculate the corresponding cross-association parameters between each polymer and water. We note that the "fictive" self-association parameters of the carbonyl groups are only used to estimate cross-interaction parameters. Under the imposed physical condition $N^{B_p} = 0$, the set of equation (6) does not introduce any association involving the "fictive" proton donor on a generic polymer carbonyl group, both in the pure polymer case (i.e., no polymer self-association occurs) and in the polymer penetrant mixture (i.e., no cross-interactions involving such fictive PD occur). Regarding the involvement of other sites on polymer backbones in possible interactions with water molecules (e.g., ether groups on PEI and 6FDA-ODA repeating units), previous in situ FT-IR investigations [47] and DFT calculation analyses (see Section 4.1.3) on the three investigated polyimides showed water molecules preferentially interact with carbonyl groups within the investigated concentration range. Specific cross-interactions with other groups present on the macromolecules were then ruled out.

4.1.2. *Glassy polyimides/H_2O binary systems*

Once the pure component as well as the self and cross interaction parameters have been estimated, only the pairwise "mean-field" binary interaction parameter, k_{ij}, needs to be determined to calculate the penetrant solubility. The literature generally reports a slight variation of k_{ij} with temperature. To account for this, a linear dependence of the binary interaction parameter on temperature is usually introduced using the following equation [40]:

$$k_{ij} = k_{ij,0} + \alpha_T\, T \tag{19}$$

$k_{ij,0}$ and α_T of eq. (19) are treated as adjustable parameters to fit thermodynamic sorption isotherms at different temperatures. Trivially, the coefficient α_T is imposed to be equal to 0 when experimental data are at only one temperature. Since, in the case of 6FDA-ODA and 6FDA-6FpDA, experimental data are available at only one value of temperature, the coefficient α_T, for these polymers, has been then imposed to be equal to 0. A satisfactory data fitting (see Fig. 3) has been obtained using NETGP-PC-SAFT to interpret previously collected solubility isotherms [35,46,47] (the best fitting values of $k_{ij,0}$ and α_T are reported in Table 2).

Once the "mean-field" interaction parameters have been estimated, the NETGP-PC-SAFT model can be used, under the IE assumption, to predict the association set $\boldsymbol{x}$ through eq. (6). Based on stoichiometry considerations, $\boldsymbol{x}$ allows, in turn, the determination of the concentration of self- and cross-specific interactions established within the polymer/penetrant glassy phase as a function of temperature and concentration at the given out-of-equilibrium polymer density. In particular, the moles of self- and cross-associations per mass of polymer, $\frac{n_{11}}{m_p}$ and $\frac{n_{12}}{m_p}$, respectively, can be calculated for the three systems investigated as:

$$\frac{n_{11}}{m_p} = \frac{N^{A_1}\left(1 - x^{A_1}\right)}{Mw_1\, N_A}\frac{\rho_1}{\rho_p} \tag{20.a}$$

$$\frac{n_{12}}{m_p} = \frac{N^{A_p}\left(1 - x^{A_p}\right)}{Mw_p\, N_A} \tag{20.b}$$

where N_A is the Avogadro's number. With reference to eq. (20), the

Table 1
PC-SAFT pure component parameters.

Species	σ_i (Å)	$\frac{\varepsilon_i}{k_B}$ (K)	m_i	$\frac{\varepsilon^{A_iB_i}}{k_B}$ (K)	$k^{A_iB_i}$	N^{A_i}	N^{B_i}	Ref.
H_2O	σ_i (T)[a]	160.9	1.72	1812	0.144	2	2	This work
PEI	3.385	366	$0.02957 \times Mw_{mol}$[b]	1000	0.1	$8\frac{Mw}{Mw_{ru}}$	0	This work
6FDA-ODA	3.057	269	$0.03076 \times Mw_{mol}$[b]	1000	0.1	$8\frac{Mw}{Mw_{ru}}$	0	This work
6FDA-6FpDA	3.065	247	$0.02466 \times Mw_{mol}$[b]	1000	0.1	$8\frac{Mw}{Mw_{ru}}$	0	This work

Mw_{ru} is the molecular weight of the repeating unit.
[a] $\sigma_i(T) = 2.348 + 0.360\exp(-0.00672\,T) + 0.0265\exp(0.00300\,T)$
[b] Molar weight of PEI, 6FDA-ODA and 6FDA-6FpDA are 80000 g/mol, 100000 g/mol, and 100000 g/mol, respectively.

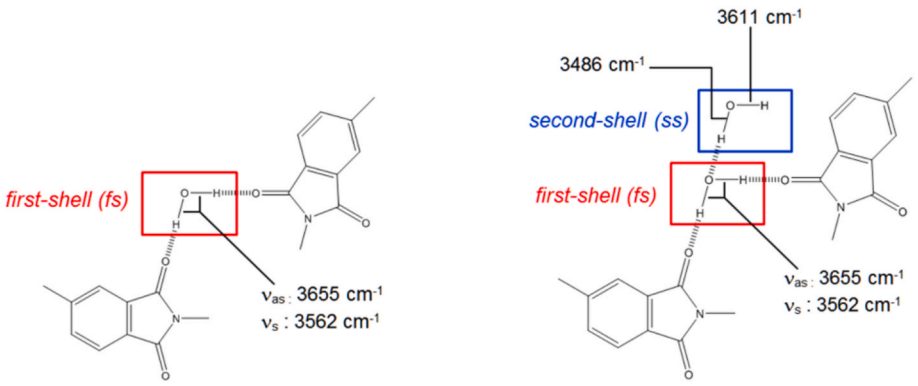

Scheme 2. Types of water molecules identified spectroscopically with the frequency of the corresponding peaks.

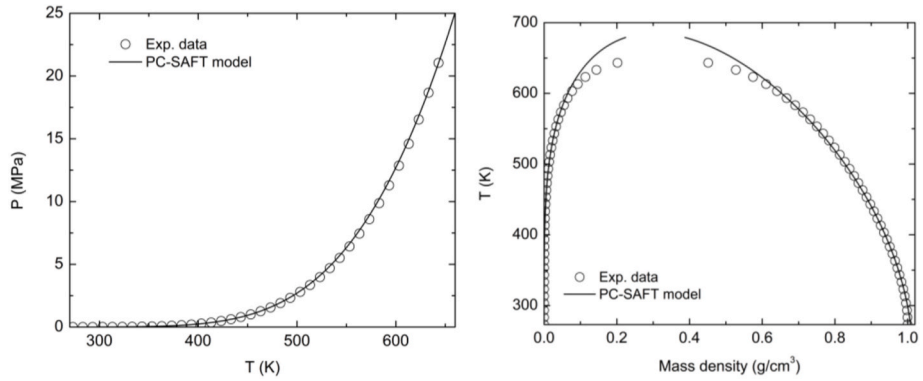

Fig. 1. Comparison between the experimental data and the fitting results for pure component parameters of water: saturation pressures (left) and saturation densities (right).

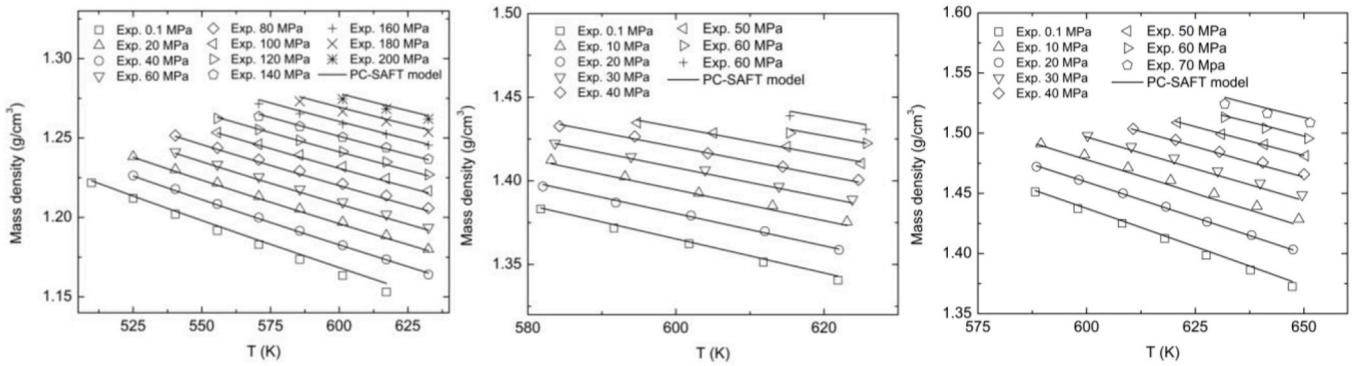

Fig. 2. Comparison between the experimental dilatometric data and the fitting results for pure component parameters of: PEI (left), 6FDA-ODA (middle) and 6FDA-6FpDA (right).

oxygen atom of the water molecule has two equivalent types of PA sites, which are described by the same association parameters. The two components of the $\boldsymbol{x}$ vector have the same value, which is indicated as x^{A_1}. Similarly, x^{A_p} represents the components of $\boldsymbol{x}$ associated with all equivalent PA sites of the oxygen atoms in the carbonyl groups on the polymer backbone. Once again, a unique value of x^{A_p} is obtained since the corresponding PA sites are consistently described by the same pair of association parameters.

In the PC-SAFT framework (and therefore in the NETGP-PC-SAFT), each type of association site is uniquely associated with one species in the system. Thus, the i-th component of x represents the number of association sites of type i that are not involved in association, relative to their total number and, equivalently, to the total number of molecules of the species that intrinsically display that type of association site [41,42]. Thus, $N^{A_1}\left(1-x^{A_1}\right)$ and $N^{A_p}\left(1-x^{A_p}\right)$ represent the total number of water PA groups and polymeric PA groups involved in specific interactions, respectively, per the total number of water and polymeric molecules. Finally, since the polymeric species do not exhibit PD groups, Eq. (20) trivially holds.

Once the pure and binary parameters have been retrieved, eq. (20) can be used to predict the self- and cross-interactions of the penetrant within the glassy polymer/penetrant system. Fig. 4 shows a satisfactory comparison between the model predictions and the experimental data taken from Ref. [47] for the three polyimides investigated. Only in the case of PEI is the agreement less satisfactory. Specifically, an overestimation of the cross-interactions is observed at the highest activities,

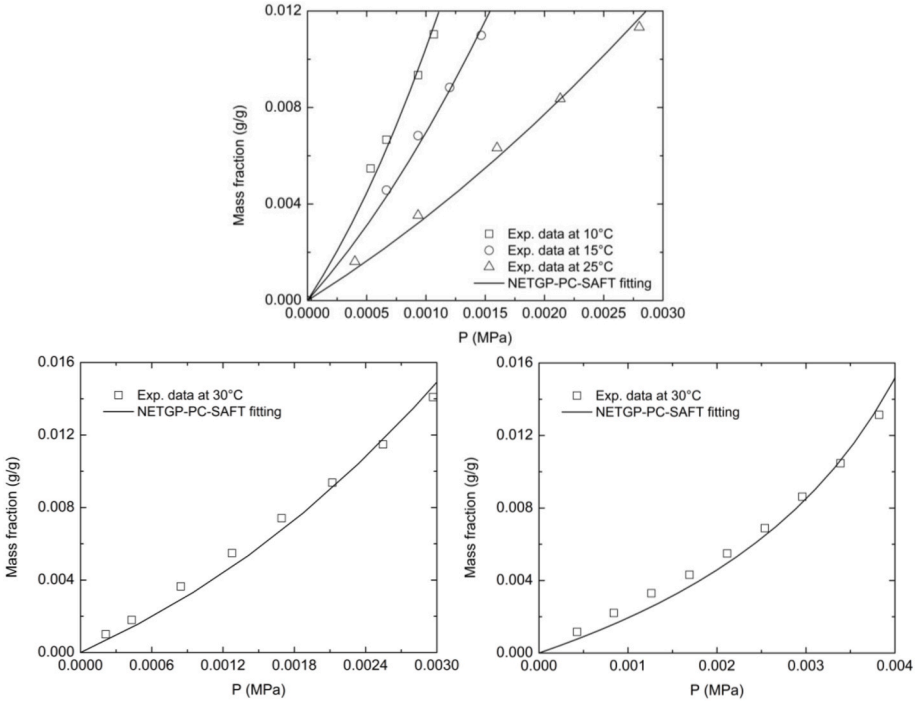

Fig. 3. Comparison between the experimental data and best fitting results by NETGP-PC-SAFT model for the glassy systems: PEI/H_2O (top, at T = 10 °C, 15 °C, 25 °C), 6FDA-ODA/H_2O (bottom left, at T = 30 °C) and 6FDA-6FpDA/H_2O (bottom right, at T = 30 °C).

Table 2
Polyimides/water PC-SAFT binary "mean-field" parameter.

Species	$k_{ij,0}$	α_T (K^{-1})	Ref.
PEI	0.234	-0.586×10^{-3}	This work
6FDA-ODA	0.0399	0[a]	This work
6FDA-6FpDA	0.140	0[a]	This work

[a] Fixed values since sorption isotherm is available only at a single temperature.

Table 3
PEI/H_2O mobility parameter.

$L^*_{1p,0}$ ($cm^2\ s^{-1}$)	β^*_1	γ_1	Ref.
2.79×10^{-8}	27.46	9.64×10^{-3}	This work

while a slight underestimation of the self-contacts is evident across the entire activity range. Previously performed molecular dynamics (MD) simulations [48] also showed a similar overestimation of the cross-association contacts. Previous modelling using a glassy, non-equilibrium, lattice-fluid (NETGP-NRHB) model under the IE assumption [44,48] displayed the same kind of deviation between theoretical predictions and experimental data.

The discrepancies highlighted here between the experimental data and both continuous thermodynamics modeling and MD calculations can be attributed to the heterogeneous structure [83] of the glassy polymeric matrix, in terms of distribution of mass density. The NETGP approach operates under the assumption of a spatial homogeneous out-of-equilibrium mass density [36,37] for the polymeric mixture. In contrast, the MD has been implemented in a simulation box that mimics the average mass density of the glassy mixture [48].

4.1.3. DFT results

To thoughtful investigate first shell PEI-H_2O coordination, different H-bond acceptor sites have been tested (i.e., sp^3 and sp^2 oxygen atoms of PEI) as well as different orientations. The most stable calculated structures are reported in Fig. 5. The obtained results show quite clearly that coordination of water to PEI preferentially occurs through the carbonyl oxygens of PEI, as reported in Fig. 5-a. Even if coordination through etheric oxygens appears to be energetically possible, it is far less favoured, having an interaction energy around −5.6 kJ/mol (see Fig. 5-b). In fact, the most stable PEI-H_2O minimum (see Fig. 5-a) shows an HB distance of 1.95 Å and a first shell water coordination energy, $E_{PEI/H2O}$, around −12.5 kJ/mol.

The DFT results are consistent with both in situ FT-IR and MD outcomes [48], pointing to a preferential coordination of the water molecules through the carbonyl groups of the repeating units of the PEI. Moreover, the first shell PEI/water coordination energy confirms the reliability of Marshall et al. [82] procedure as the resulting cross-HB interaction energy, calculated through eq. (4) and adopted in NETGP-PC-SAFT model, is 11.7 kJ/mol, close to the absolute value of the first shell coordination energy. In fact, we underline here that the interaction energies of NETGP-PC-SAFT model are intrinsically defined as the opposite of the coordination energies.

Since the repeating units of the three polyimides under investigation display the same types of groups potentially involved in the specific interaction with water molecules and in view of the local nature of the hydrogen bonding, it is expected that the three polyimides have similar coordination energies for the first shell populations. Indeed, such a feature is consistent with the implementation of eq. (4) in the NETGP-PC-SAFT modelling.

4.2. Sorption kinetics of H_2O in glassy PEI

4.2.1. In situ FT-IR

For the present investigation, we have developed a specific procedure to quantify water sorption kinetics accounting for the occurrence of possible different penetrant populations [48]. Such procedure is based upon in situ FT-IR analysis focused on the ν(OH) range (3800–3200 cm^{-1}) where absorbed water displays its more characteristic and intense signals. The sorbate spectrum was isolated by difference spectroscopy, removing the interference of the polymer matrix in the region of interest [48,84]. The resulting profile is reported in Fig. 6A as it evolves with

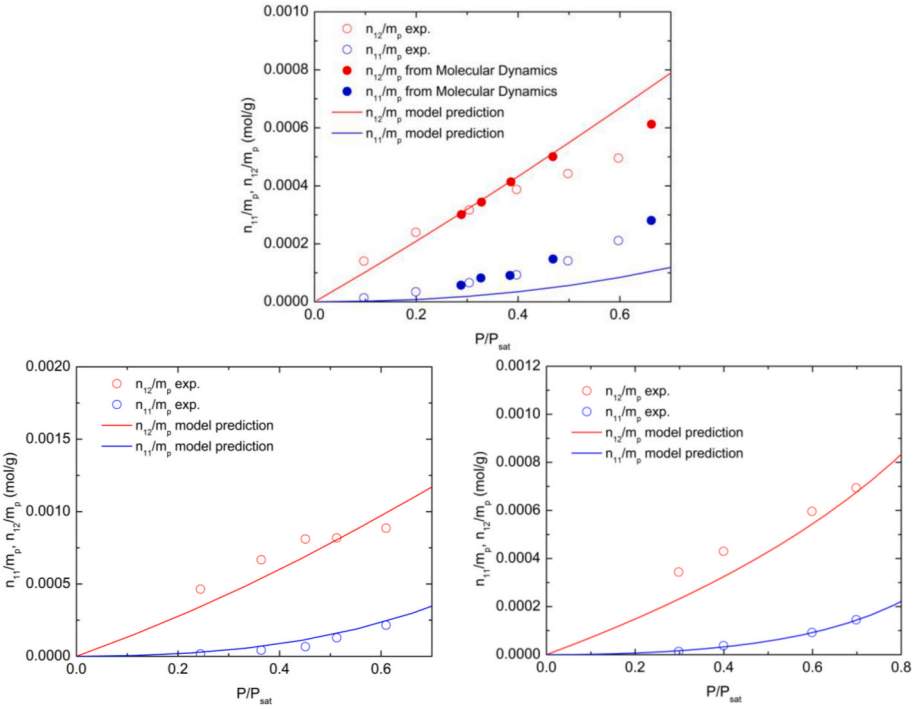

Fig. 4. Moles of self- and cross-interactions of the penetrant itself and with the polymer, respectively. Comparison between the experimental data and the predictions by NETGP-PC-SAFT model for the systems: PEI/H_2O (top, at T = 30 °C), 6FDA-ODA/H_2O (bottom left, at T = 30 °C) and 6FDA-FpDA/H_2O (bottom right, at T = 30 °C).

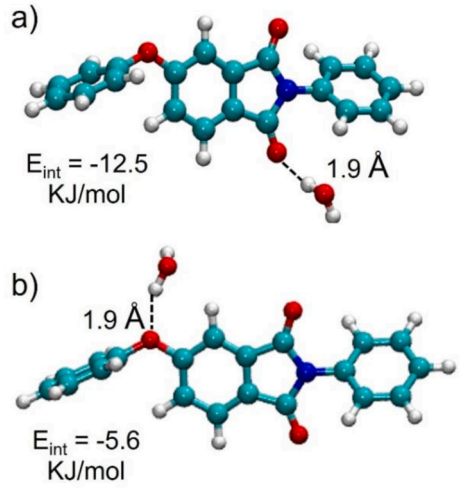

Fig. 5. Fully optimized structures for PEI/H_2O adducts. Hydrogen atoms are in white, carbon atoms are in green, oxygens are in red, and nitrogen atoms are in blue. Important distances and interaction energies are also reported. (For interpretation of the references to colour in this figure legend, the reader is referred to the Web version of this article.)

time during the integral sorption experiment at P/P_{sat} = 0.6. Fig. 6B displays the Least-squares Curve fitting analysis (LSCF) of a typical spectrum.

The interpretation of the multicomponent bandshape has been achieved with the aid of 2D-correlation spectroscopy and has been discussed in detail in Ref. [48]. We summarize here the essential results relevant to the forthcoming discussion. Two couples of signals evolving synchronously were identified at 3655–3562 cm^{-1} and at 3611–3486 cm^{-1}; the first doublet is due to the symmetric and antisymmetric stretching of water molecules H-bonded to imide carbonyls. In particular, spectroscopic evidence and molecular dynamics (MD) simulations [48] demonstrated that this bonding has a 1:2 stoichiometry, i.e. is of the type C═O···HOH···O═C, bridging, the carbonyls belonging to two consecutive imide group present on a PEI macromolecule. The second doublet originates from water molecules self-associated to water molecules H-bonded to imide carbonyls, forming a dimer. A schematic representation of the molecular aggregates identified spectroscopically, along with the frequency of the peaks they produce, is reported in Scheme 2.

By coupling the results of water sorption isotherms measured spectroscopically and gravimetrically, it was possible to evaluate the molar absorptivities of the *first-shell (fs)* and the *second-shell (ss)* water molecules (ε_{fs}, ε_{ss}) according to the method developed in Ref. [84]. These were found to be 34.5 km/mol and 89.7 km/mol, respectively [48]. These values allowed us to estimate the volumetric concentration of the two populations from the integrated absorbance of the bandshape components resolved by the LSCF analysis. In particular, C_{fs}=$A_{fs}/\xi\ \varepsilon_{fs}$ and C_{ss}=$A_{ss}/\xi\ \varepsilon_{ss}$, where A_{fs} and A_{ss} are the integrated absorbances of the components at 3562 and 3486 cm^{-1}, respectively (see Fig. 6B).

The results of the kinetic analysis in terms of the average concentration of penetrant and the average concentration of *fs* and *ss* molecules are presented in Fig. 7. It is found that the concentration of water molecules directly interacting with the polymer matrix grows faster and reaches higher equilibrium values than the concentration of those belonging to the second shell. Further details on this experimental procedure can be found in Ref. [47].

4.2.2. *Modelling of sorption kinetics*

Once the set of parameters of the NETGP-PC-SAFT model which rules the solubility modelling for the binary PEI/H_2O system have been obtained, the NETGP-PC-SAFT-SD model has been adopted to investigate the implications of the IE assumption for water sorption kinetics in such glassy system. As previously outlined, the IE equilibrium hypothesis introduced when dealing with the phase pseudo-equilibrium case, is now adopted, in a more general manner, during the sorption kinetics process at any given time and at any spatial point of the glassy mixture.

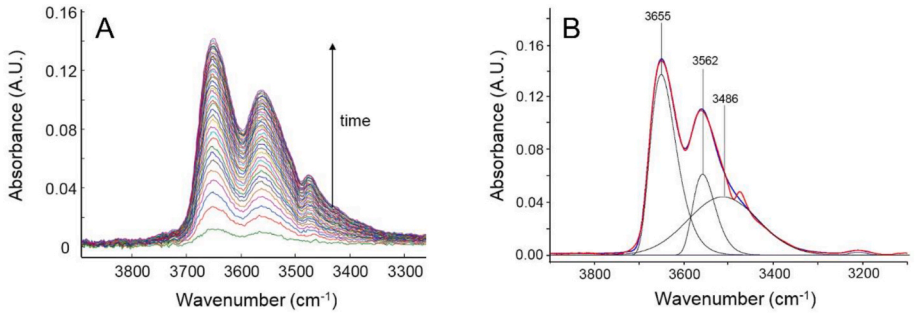

Fig. 6. (A) Spectrum of sorbed H_2O collected at increasing times (0–160 s) during the sorption experiment at $P/P_{sat} = 0.6$. (B) Curve fitting analysis of the profile collected at sorption equilibrium.

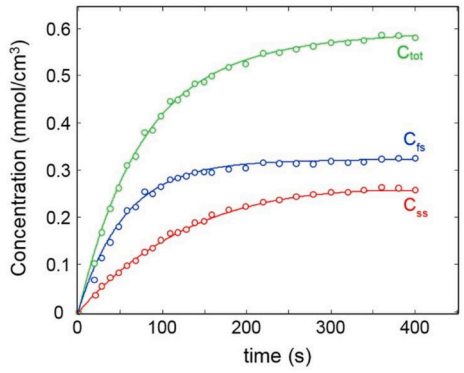

Fig. 7. Volumetric average concentration of respectively sorbed water (green dots), first-shell H_2O (blue dots) and second-shell H_2O (red dots) as a function of time for the sorption experiment at $P/P_{sat} = 0.6$. Connecting curves are for eye guidance. (For interpretation of the references to colour in this figure legend, the reader is referred to the Web version of this article.)

This stronger assumption has been here successfully validated against kinetics FT-IR outcomes for the first time in the existing literature. To this end, as explained in section 3.2, it is necessary to retrieve the additional set of mass transport parameters, $L^*_{1p,0}$, β^*_1 and γ_1, which allows the determination of the mobility factor for the investigated isothermal case.

These parameters were estimated through a fitting procedure performed on isothermal sorption kinetics of water in PEI collected for the present investigation by in situ FT-IR spectroscopy. An integral sorption test was conducted from dry condition up to $P/P_{sat} = 0.6$ at 30 °C to better estimate the concentration effect on the mobility factor. As demonstrated in Fig. 8, the model provides an excellent fitting of the experimental data, expressed as the total mass of water sorbed at time t with respect to the value of water sorbed at the pseudo-equilibrium (M_t/M_∞). Indeed, the solution to the PDE problem delineated in Section 3.2 furnishes the penetrant mass concentration profile at any given experimental instant in time. This profile can be integrated numerically across the entire domain of the glassy mixtures in order to obtain the time evolution of M_t/M_∞. In Table 3 are reported the optimized values of the fitting parameters.

Based on the stoichiometry suggested by FT-IR analysis as well by MD calculations, the time-evolution of the average concentration of self- and cross-contacts per total mass of polymer $\frac{n_{11}}{m_p}$ and $\frac{n_{12}}{m_p}$ can be trivially obtained by the experimentally determined kinetics curves of *fs* and *ss* water molecules. In fact, each *ss* water molecule is univocally associated to a self-association contact (n_{11}) and each *fs* water molecule is univocally associated to two cross-association contacts (n_{12}). On the other hand, the solution of the PDE problem discussed in section 3.2 provides, as side result, also the profiles of x^{A_1} and x^{A_p} at any given instant of time that, when inserted in eq. (20), allow to determine at any instant of time t the volumetric concentration profile of the number of moles of self and cross interactions c_{11} and c_{12}, since $c_{ij} = \frac{n_{ij}}{m_p}\rho_p$ (i = 1; j = 1,2). In the one-dimensional case considered, such two spatial profiles can be numerically integrated at each t to obtain the time evolution of n_{11}/S and n_{12}/S (S being the area of the sample film orthogonal to the thickness direction), so that, the normalized kinetics $n_{11}/n_{11,\infty}$ and $n_{12}/n_{12,\infty}$ are trivially obtained. The symbol ∞ refers here to the value obtained integrating the pseudo-equilibrium (spatial uniform) profile.

In Fig. 9 the NETGP-PC-SAFT-SD model predictions, obtained by this procedure in correspondence of the optimized fitting parameters, are compared with the experimental data, in terms of values normalized with respect to the corresponding values attained at the pseudo-equilibrium conditions. Model predictions are in a very good agreement with data, despite the absolute values of the self- and cross-

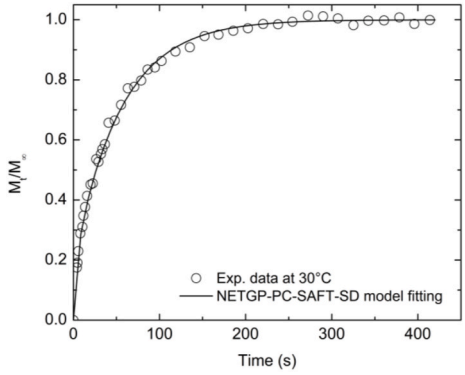

Fig. 8. Comparison between experimental integral kinetics sorption isotherm at 30 °C (external activity step from 0 to 0.6) and the NETGP-PC-SAFT-SD best fitting curve.

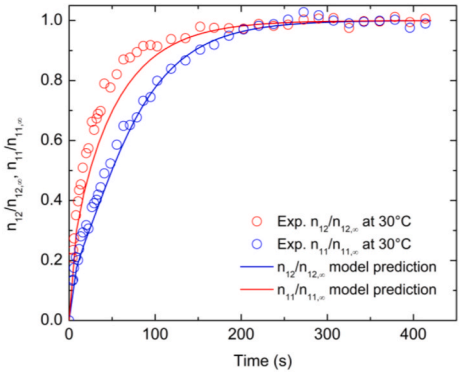

Fig. 9. Comparison between experimental normalized kinetics evolution of self- and cross-specific interactions at 30 °C and the NEGTP-PC-SAFT-SD model prediction.

contacts in correspondence of the isothermal pseudo-equilibrium conditions displays a mismatch with the experimental values, as shown in Fig. 4 top. Indeed, such feature indicate that the model, under IE assumption, is able to reproduce the dynamics of the water sorption mechanism, but, likely, the number of effective interacting sites available for the contacts is lower than the ideal ones adopted in the modelling on the basis of polymer structure, thus resulting in the observed overestimation of specific cross-contacts and, consequently, the underestimation of the self-contacts provided by the model.

5. Conclusions

The sorption thermodynamics of water in glassy amorphous PEI, 6FDA-ODA, and 6FDA-6FpDA have been adequately described by adopting a multiscale and multidisciplinary approach. In particular, it has been determined that in situ FT-IR experiments and DFT calculations provide a useful guideline to properly implement a continuum thermodynamics model (NETGP-PC-SAFT with associative term) specifically developed in literature to account simultaneously for the out-of-equilibrium state of the polymer-penetrant mixtures and for a complex interactional scenario, displaying both self- and cross-Hydrogen Bonding interactions.

To this end, the FT-IR and DFT indications have been utilized to accurately account for the type of associative sites for each binary system in the implementation of the NETGP-PC-SAFT model. The model has demonstrated an exemplary correlation capacity in terms of H_2O solubility for each system that has been examined. In this context, the present investigation has focused on the implications of the Instantaneous Equilibrium assumption for the associative contacts in the NETGP-PC-SAFT framework, whose reliability has not been yet directly assessed in literature. In fact, employing the optimized “mean field” parameters in conjunction with the mixing rule for the cross-interaction energy (an approach further substantiated by DFT calculations) has enabled the effective prediction of the cross- and self-interactions for the three systems under investigation. Indeed, the model results closely resemble the outcomes of in situ FT-IR spectroscopy, obtained using a specific experimental procedure that has been developed previously. Furthermore, for the PEI/H_2O system, the prediction of specific contacts has also been adequately validated against the MD outcomes reported in the same previous studies.

Following a comprehensive evaluation of the NETGP-PC-SAFT capability, including a microscopic analysis, the potential implementation of this model within the general Standard Diffusion framework has been explored. This implementation would enable the self-consistent description of water sorption kinetics in glassy systems exhibiting a complex interactive scenario. To this end, the NETGP-PC-SAFT-SD model has been implemented to investigate the water sorption kinetics in the PEI/H_2O amorphous glassy system. In this regard, a self-consistent constitutive equation has been proposed, drawing inspiration from the "free-volume" concept, to model the dependence of the mobility factor on water concentration. This modeling approach has demonstrated a remarkable correlation capability in the context of water sorption kinetics.

Finally, the NETGP-PC-SAFT-SD has been utilized to predict the sorption kinetics of the cross- and self-association concentration displaying an excellent agreement with the results of in situ FT-IR spectroscopy, obtained using a procedure specifically developed in the present contribution to determine the kinetics of different H_2O populations in amorphous PEI. The validation of the kinetic model indicates that the Instantaneous Equilibrium assumption for H_2O/H_2O and H_2O/PEI Hydrogen Bonding is reasonable, not only when dealing with pseudo phase equilibrium conditions but also for describing water sorption kinetics.

The integration of the NETGP-PC-SAFT and Standard Diffusion models to describe population-specific kinetics, as illustrated, represents a significant advancement. This approach has potential implications in predicting the performance of glassy polymers in specific membrane separation processes involving water molecules or in the rational design of polymers with tailored moisture barrier properties. With particular emphasis on polyimides, pertinent commercial applications in which this approach can be utilized include the removal of water vapor from natural gas and other gases, the separation of water from water-alcohols mixtures, the pervaporation dehydration of organic liquids, and the recovery or removal of organics from water.

CRediT authorship contribution statement

C. Brondi: Writing – original draft, Software, Methodology. **A. Correa:** Software, Investigation. **G. Mensitieri:** Writing – review & editing, Supervision, Project administration. **P. Musto:** Investigation, Data curation. **S. Scala:** Writing – review & editing, Data curation. **G. Scherillo:** Writing – original draft, Validation, Formal analysis. **A. Baldanza:** Writing – original draft, Software, Investigation.

Declaration of competing interest

The authors declare that they have no known competing financial interests or personal relationships that could have appeared to influence the work reported in this paper.

Appendix A. Supplementary data

Supplementary data to this article can be found online at https://doi.org/10.1016/j.polymer.2026.129604.

Data availability

Data will be made available on request.

References

[1] R. Bernstein, Y. Kaufman, V. Freger, Membrane characterization, in: E.M.V. Hoek, V.V. Tarabara (Eds.), Encyclopedia of Membrane Science and Technology, first ed., Wiley-Blackwell, Hoboken, NJ, USA, 2013. ISBN 978-0-470-90687-3.
[2] A. Brunetti, G. Barbieri, E. Drioli, Gas separation, applications, in: E.M.V. Hoek, V. V. Tarabara (Eds.), Encyclopedia of Membrane Science and Technology, first ed., Wiley-Blackwell, Hoboken, NJ, USA, 2013. ISBN 978-0-470-90687-3.
[3] W.J. Koros, G.K. Fleming, S.M. Jordan, T.H. Kim, H.H. Hoehn, Polymeric membrane materials for solution-diffusion based permeation separations, Prog. Polym. Sci. 13 (1988) 339–401, https://doi.org/10.1016/0079-6700(88)90002-0.
[4] W.J. Koros, S.K. Burgess, Z. Chen, Polymer transport properties, in: Encyclopedia of Polymer Science and Technology, fourth ed., John Wiley & Sons, Hoboken, NJ, USA, 2015. ISBN 9781118633892.
[5] G. Mensitieri, M. Iannone, Modelling accelerated ageing in polymer composites, in: R. Martin (Ed.), Ageing of Composites, first ed., Woodhead Publishing, Ltd.: Cambridge, UK; CRC Press, Boca Raton, FL, USA, 2008, pp. 224–281. ISBN 9781845693527.
[6] J. Glass, Adsorption characteristics of water-soluble polymers. I. Poly(vinyl alcohol) and poly(vinylpyrrolidone) at the aqueous-air interface, J. Phys. Chem. 72 (1968) 4450–4458, https://doi.org/10.1021/j100859a014.
[7] C. Sammon, C. Mura, J. Yarwood, N. Everall, R. Swart, D. Hodge, FTIR ATR studies of the structure and dynamics of water molecules in polymeric matrixes. A comparison of PET and PVC, J. Phys. Chem. B 102 (1998) 3402–3411, https://doi.org/10.1021/ma00103a013.
[8] N.A. Belova, A.P. Safronov, Y.P. Yampolskii, Inverse gas chromatography and the thermodynamics of sorption in polymers, Polym. Sci. 54 (2012) 859–873, https://doi.org/10.1134/s0965545x1210001x.
[9] E.M. Davis, Y.A. Elabd, Prediction of water solubility in glassy polymers using nonequilibrium thermodynamics, Ind. Eng. Chem. Res. 52 (2013) 12865–12875, https://doi.org/10.1021/ie401713h.
[10] R. Iwamoto, H. Kusanagi, Hydration structure and mobility of the water contained in Poly(ethylene terephthalate), J. Phys. Chem. A 119 (2015) 2885–2894, https://doi.org/10.1021/acs.jpca.5b00385.
[11] C.G. Panayiotou, K.S. Birdi, Handbook of Surface and Colloid Chemistry, third ed., CRC Press Taylor and Francis Group, New York, NY, USA, 2009.
[12] G.M. Kontogeorgis, G.K. Folas, Thermodynamic Models for Industrial Applications: from Classical and Advanced Mixing Rules to Association Theories, 1sted., John Wiley&Sons, Ltd., Chichester, UK, 2010. ISBN978-0-470-69726-9.
[13] M.G. De Angelis, G.C. Sarti, Solubility of gases and liquids in glassy polymers, Annu. Rev. Cell Biol. 2 (2011) 97–120, https://doi.org/10.1146/annurev-chembioeng-061010-114247.

[14] E. Chiessi, F. Cavalieri, G. Paradossi, Water and polymer dynamics in chemically cross-linked hydrogels of Poly(vinyl alcohol): a molecular dynamics simulation Study, J. Phys. Chem. B 111 (2007) 2820–2827, https://doi.org/10.1021/jp0671143.
[15] Z.-J. Zhao, Q. Wang, L. Zhang, T. Wu, Structured water and Water—Polymer interactions in hydrogels of molecularly imprinted polymers, J. Phys. Chem. B 112 (2008) 7515–7521, https://doi.org/10.1021/jp800836d.
[16] H. Eslami, F. Müller-Plathe, Molecular dynamics simulation of water influence on local structure of nanoconfined Polyamide-6,6, J. Phys. Chem. B 115 (2011) 9720–9731, https://doi.org/10.1021/jp204423z.
[17] L.M. Robeson, Polymer membranes for gas separation, Curr. Opin. Solid State Mater. Sci. 4 (1999) 549–555.
[18] I. Merdas, F. Thominette, J. Verdu, Humid ageing of polyetherimide. Chemical and physical interactions with water, in: K.L. Mittal (Ed.), Polyimides and Other High Temperature Polymer: Synthesis, Characterization and Applications, VSP: Utrecht, the Netherlands, vol. 2, 2003, pp. 255–266. ISBN 90-6764-378-5.
[19] M. Karimi, W. Albrecht, M. Heuchel, M.H. Kish, J. Frahn, T. Weigel, D. Hofmann, H. Modarress, A. Lendlein, Determination of water/polymer interaction parameter for membrane-forming systems by sorption measurement and a fitting technique, J. Membr. Sci. 265 (2005) 1–12, https://doi.org/10.1016/j.memsci.2005.04.030.
[20] J. Seo, W. Jang, H. Han, Thermal, optical, and water sorption properties in composite films of poly(ether imide) and bismaleimides: effect of chemical structure, J. Appl. Polym. Sci. 113 (2009) 777–783, https://doi.org/10.1002/app.29694.
[21] R. Checchetto, M. Scarpa, M.G. De Angelis, M. Minelli, Mixed gas diffusion and permeation of ternary and quaternary CO_2/CO/N_2/O_2 gas mixtures in matrimid®, polyetherimide and poly (lactic acid) membranes for CO_2/CO separation, J. Membr. Sci. 659 (2022) 120768, https://doi.org/10.1016/j.memsci.2022.120768.
[22] G.V. Sarrigani, J. Ding, A.E. Ghadi, D. Alam, P. Fitzgerald, D.E. Wiley, D.K. Wang, Interfacially-confined polyetherimide tubular membranes for H_2, CO_2 and N_2 separations, J. Membr. Sci. 655 (2022) 120596, https://doi.org/10.1016/j.memsci.2022.120596.
[23] Y. Guo, W. Zhao, D. Li, J. Liu, J. Qian, L. Pang, T. Zhou, W. Liu, Z. Liu, H. Huang, J. Zhai, D. Zhou, Ultra-High capacitive energy storage density at 150° C achieved in polyetherimide composite films by filler and structure design, Adv. Mater. 37 (2025) 2415652, https://doi.org/10.1002/adma.202415652.
[24] C. Pavlou, N. Koutroumanis, A.C. Manikas, M.G. Pastore Carbone, G. Paterakis, C. Galiotis, Highly efficient, electro-thermal heater based on Marangoni-Driven, oriented reduced graphene Oxide/Poly (ether imide) nanolaminates, ACS Appl. Mater. Interfaces 17 (2024) 2000–2009, https://doi.org/10.1021/acsami.4c17273.
[25] K. Tanaka, H. Kita, M. Okano, K. Okamoto, Permeability and permselectivity of gases in fluorinated and non-fluorinated polyimides, Polymer 33 (1992) 585–592, https://doi.org/10.1016/0032-3861(92)90736-G.
[26] J.D. Wind, C. Staudt-Bickel, D.R. Paul, W.J. Koros, The effects of crosslinking chemistry on CO_2 plasticization of polyimide gas separation membranes, Ind. Eng. Chem. Res. 41 (2002) 6139–6148, https://doi.org/10.1021/ie0204639.
[27] P. Jia, J. Liu, J. Kong, M. Hu, N. Qi, Z. Chen, Shan Xu, N. Li, Tailoring the micropore structure of 6FDA-based polyimide membrane for gas permselectivity studied by positron annihilation, Sep. Purif. Technol. 282 (2022) 120044, https://doi.org/10.3390/membranes13050461.
[28] J. Tan, Y. Chen, J. Huang, L. Jiang, L. Fei, W. Sun, D. Wu, H. Zhang, Y. Liu, Influence of diamine moieties on the gas permeation performances of polyimide: perspectives from experiment and simulation, J. Polym. Res. 30 (2023) 317, https://doi.org/10.1007/s10965-023-03677-8.
[29] H. Yanagishita, C. Maejima, D. Kitamoto, T. Nakane, Preparation of asymmetric polyimide membrane for water/ethanol separation in pervaporation by the phase inversion process, J. Membr. Sci. 86 (1994) 231–240, https://doi.org/10.1016/0376-7388(93)E0147-C.
[30] H. Yanagishita, D. Kitamoto, T. Nakane, Separation of alcohol aqueous solution by pervaporation using asymmetric polyimide membrane, High Perform. Polym. 7 (1995) 275–281, https://doi.org/10.1088/0954-0083/7/3/004.
[31] X. Feng, R.Y.M. Huang, Pervaporation and performance of asymmetric polyetherimide membranes for isopropanol dehydration by pervaporation, J. Membr. Sci. 109 (1996) 165–172, https://doi.org/10.1016/0376-7388(95)00198-0.
[32] S.I. Semenova, Separation properties of polyimides, in: H. Ohya, V.V. Kudryavsev, S.I. Semenova (Eds.), Polyimide Membranes-Applications, Fabrications, and Properties, Kodansha, Tokyo, Japan, 1996, pp. 103–178. ISBN 4-06-208189-X.
[33] W. Qiu, M. Kosuri, F. Zhou, W.J. Koros, Dehydration of ethanol–water mixtures using asymmetric hollow fiber membranes from commercial polyimides, J. Membr. Sci. 327 (2009) 96–103, https://doi.org/10.1016/j.memsci.2008.11.029.
[34] G. Scherillo, L. Sanguigno, M. Galizia, M. Lavorgna, P. Musto, G. Mensitieri, Non-equilibrium compressible lattice theories accounting for hydrogen bonding interactions: modelling water sorption thermodynamics in fluorinated polyimides, Fluid Phase Equilib. 334 (2012) 166–188, https://doi.org/10.1016/j.fluid.2012.06.030.
[35] A. Baldanza, C. Brondi, V. Loianno, G. Mensitieri, G. Scherillo, Modelling relative humidity and temperature effects on CO_2 gas transport in polyetherimide, Polymer 291 (2024) 126595, https://doi.org/10.1016/j.polymer.2023.126595.
[36] F. Doghieri, G.C. Sarti, Nonequilibrium lattice fluid: a predictive model for the solubility in glassy polymers, Macromolecules 29 (1996) 7885–7896, https://doi.org/10.1021/ma951366c.
[37] G.C. Sarti, F. Doghieri, Predictions of the solubility of gases in glassy polymers based on the NELF model, Chem. Eng. Sci. 53 (1998) 3435–3447, https://doi.org/10.1016/S0009-2509(98)00143-2.
[38] M.G. De Angelis, F. Doghieri, G.C. Sarti, B.D. Freeman, Modeling gas sorption in amorphous Teflon through the non equilibrium thermodynamics for glassy polymers (NET-GP) approach, Desalination 193 (2006) 82–89, https://doi.org/10.1016/j.desal.2005.06.057.
[39] E.M. Davis, Y.A. Elabd, Water clustering in glassy polymers, J. Phys. Chem. B 117 (2013) 10629–10640, https://doi.org/10.1021/jp405388d.
[40] L. Liu, S.E. Kentish, Modeling of carbon dioxide and water sorption in glassy polymers through PC-SAFT and NET PEC-SAFT, Polymer 104 (2016) 149–155, https://doi.org/10.1016/j.polymer.2016.10.002.
[41] W.G. Chapman, K.E. Gubbins, G. Jackson, M. Radosz, New reference equation of state for associating liquids, Ind. Eng. Chem. Res. 29 (1990) 1709–1721, https://doi.org/10.1021/ie00104a021.
[42] M.L. Michelsen, E.M. Hendriks, Physical properties from association models, Fluid Phase Equilib. 180 (2001) 165–174, https://doi.org/10.1016/S0378-3812(01)00344-2.
[43] F. Tumakaka, J. Gross, G. Sadowski, Thermodynamic modeling of complex systems using PC-SAFT, Fluid Phase Equilib. 228–229 (2005) 89–98, https://doi.org/10.1016/j.fluid.2004.09.037.
[44] G. Mensitieri, G. Scherillo, C. Panayiotou, P. Musto, Towards a predictive thermodynamic description of sorption processes in polymers: the synergy between theoretical EoS models and vibrational spectroscopy, Mater. Sci. Rep. 140 (2020) 100525, https://doi.org/10.1016/j.mser.2019.100525.
[45] A. Baldanza, C. Brondi, A. Correa, P. Musto, G. Mensitieri, G. Scherillo, Modelling sorption thermodynamics of gases, vapors and gas mixtures in glassy polymers using a non-equilibrium version of PC-SAFT accounting for specific interactions and volume change, Sep. Purif. Technol. 367 (2025) 132839, https://doi.org/10.1016/j.seppur.2025.132839.
[46] G. Scherillo, M. Petretta, M. Galizia, P. La Manna, P. Musto, G. Mensitieri, Thermodynamics of water sorption in high performance glassy thermoplastic polymers, Front. Chem. 2 (2014) 1–16, https://doi.org/10.3389/fchem.2014.00025.
[47] G. Scherillo, P. La Manna, P. Musto, G. Mensitieri, Water sorption thermodynamics in glassy polymers endowed with hydrogen bonding interactions, Sci. China Phys. Mech. Astron. 63 (2020) 247012, https://doi.org/10.1007/s11433-019-1433-3.
[48] A. De Nicola, A. Correa, G. Milano, P. La Manna, P. Musto, G. Mensitieri, G. Scherillo, Local structure and dynamics of water absorbed in poly (ether imide): a hydrogen bonding anatomy, J. Phys. Chem. B 121 (2017) 3162–3176, https://doi.org/10.1021/acs.jpcb.7b00992.
[49] M. Minelli, G.C. Sarti, Elementary prediction of gas permeability in glassy polymers, J. Membr. Sci. 521 (2017) 73–83, https://doi.org/10.1016/j.memsci.2016.09.001.
[50] E. Toni, M. Minelli, G.C. Sarti, A predictive model for the permeability of gas mixtures in glassy polymers, Fluid Phase Equilib. 455 (2018) 54–62, https://doi.org/10.1016/j.fluid.2017.09.025.
[51] B.D. Marshall, J.R. Johnson, Dry glass reference perturbation theory predictions of the pervaporation separation of solvent mixtures using PIM-1 membranes, J. Membr. Sci. 672 (2023) 121420, https://doi.org/10.1016/j.memsci.2023.121420.
[52] D. Borrmann, A. Danzer, G. Sadowski, Water sorption in glassy polyvinylpyrrolidone-based polymers, Membranes 12 (2022) 434, https://doi.org/10.3390/membranes12040434.
[53] M. Minelli, M.G. De Angelis, G.C. Sarti, Predictive calculations of gas solubility and permeability in glassy polymeric membranes: an overview, Front. Chem. Sci. Eng. 11 (2017) 405–413, https://doi.org/10.1007/s11705-017-1615-5.
[54] M. Minelli, G.C. Sarti, Gas permeability in glassy polymers: a thermodynamic approach, Fluid Phase Equilib. 424 (2016) 44–51, https://doi.org/10.1016/j.fluid.2015.09.027.
[55] A. Baldanza, V. Loianno, G. Mensitieri, G. Scherillo, Predictive approach for the solubility and permeability of binary gas mixtures in glassy polymers based on NRHB model, Ind. Eng. Chem. Res. 61 (2022) 3439–3456, https://doi.org/10.1021/acs.iecr.1c04864.
[56] J. Gross, G. Sadowski, Perturbed-Chain SAFT: an equation of State based on a perturbation theory for chain molecules, Ind. Eng. Chem. Res. 40 (2001) 1244, https://doi.org/10.1021/ie0003887.
[57] J.P. Wolbach, S.I. Sandler, Using molecular orbital calculations to describe the phase behavior of cross-associating mixtures, Ind. Eng. Chem. Res. 37 (1998) 2917–2928, https://doi.org/10.1021/ie970781l.
[58] M. Kleiner, G. Sadowski, Modeling of polar systems using PCP-SAFT: an approach to account for induced-association interactions, J. Phys. Chem. C 111 (2007) 15544–15553, https://doi.org/10.1021/jp072640v.
[59] I.C. Sanchez, R.H. Lacombe, Statistical thermodynamics of polymer solutions, Macromolecules 11 (1978) 1145–1156, https://doi.org/10.1021/ma60066a017.
[60] C. Panayiotou, I. Tsivintzelis, I.G. Economou, Nonrandom hydrogen-bonding model of fluids and their mixtures. 2. Multicomponent mixtures, Ind. Eng. Chem. Res. 46 (2007) 2628–2636, https://doi.org/10.1021/ie0612919.
[61] A. Baldanza, V. Loianno, G. Mensitieri, C. Panayiotou, G. Scherillo, On the thermodynamic consistency of non-random hydrogen bonding lattice-fluid model for multicomponent mixtures, Fluid Phase Equilib. 553 (2022) 113302, https://doi.org/10.1016/j.fluid.2021.113302.
[62] R.B. Bird, D.J. Klingenberg, Multicomponent diffusion brief review, Adv. Water Resour. 62 (2013) 238–242, https://doi.org/10.1016/j.advwatres.2013.05.010.
[63] M.H. Cohen, D. Turnbull, Molecular transport in liquids and glasses, J. Chem. Phys. 31 (1959) 1164–1169, https://doi.org/10.1063/1.1730566.

[64] H. Fujita, A. Kishimoto, K. Matsumoto, Concentration and temperature dependence of diffusion coefficients for systems polymethyl acrylate and n-alkyl acetates, Trans. Faraday Soc. 56 (1960) 424, https://doi.org/10.1039/TF9605600424.
[65] A. Correa, A. De Nicola, G. Scherillo, V. Loianno, D. Mallamace, F. Mallamace, H. Ito, P. Musto, G. Mensitieri, A molecular interpretation of the dynamics of diffusive mass transport of water within a glassy polyetherimide, Int. J. Mol. Sci. 22 (2021) 2908, https://doi.org/10.3390/ijms22062908.
[66] J. Gross, G. Sadowski, Application of the perturbed-chain SAFT equation of State to associating systems, Ind. Eng. Chem. Res. 41 (2002) 5510, https://doi.org/10.1021/ie010954d.
[67] W.J. Koros, Sorption and Transport in Glassy Polymers, The University of Texas at Austin, 1977. Ph. D. Dissertation.
[68] R.J. LeVeque, Finite Difference Methods for Ordinary and Partial Differential Equations: Steady-State and Time-dependent Problems, Society for Industrial and Applied Mathematics, Philadelphia, PA, USA, 1955. ISBN 978-0-898716-29-0.
[69] M.J. Frisch, G.W. Trucks, H.B. Schlegel, G.E. Scuseria, M.A. Robb, J.R. Cheeseman, G. Scalmani, V. Barone, B. Mennucci, G.A. Petersson, H. Nakatsuji, M. Caricato, X. Li, H.P. Hratchian, A.F. Izmaylov, J. Bloino, G. Zheng, J.L. Sonnenberg, M. Hada, M. Ehara, K. Toyota, R. Fukuda, J. Hasegawa, M. Ishida, T. Nakajima, Y. Honda, O. Kitao, H. Nakai, T. Vreven, J.A. Montgomery Jr., J.E. Peralta, F. Ogliaro, M. Bearpark, J.J. Heyd, E. Brothers, K.N. Kudin, V.N. Staroverov, R. Kobayashi, J. Normand, K. Raghavachari, A. Rendell, J.C. Burant, S.S. Iyengar, J. Tomasi, M. Cossi, N. Rega, J.M. Millam, M. Klene, J.E. Knox, J.B. Cross, V. Bakken, C. Adamo, J. Jaramillo, R. Gomperts, R.E. Stratmann, O. Yazyev, A.J. Austin, R. Cammi, C. Pomelli, J.W. Ochterski, R.L. Martin, K. Morokuma, V.G. Zakrzewski, G.A. Voth, P. Salvador, J.J. Dannenberg, S. Dapprich, A.D. Daniels, O. Farkas, J. B. Foresman, J.V. Ortiz, J. Cioslowski, D.J. Fox, Gaussian 09, Revision A.1, Gaussian, Inc., Wallingford, CT, 2009.
[70] A.D. Becke, Density-functional thermochemistry. III. The role of exact exchange, J. Chem. Phys. 98 (1993) 5648–5652, https://doi.org/10.1063/1.464913.
[71] C. Lee, W. Yang, R.G. Parr, Development of the Colle-Salvetti correlation-energy formula into a functional of the electron density, Phys. Rev. B 37 (1988) 785–789, https://doi.org/10.1103/PhysRevB.37.785.
[72] S.H. Vosko, L. Wilk, Influence of an improved local-spin-density correlation-energy functional on the cohesive energy of alkali metals, Phys. Rev. B 22 (1980) 3812, https://doi.org/10.1103/PhysRevB.22.3812.
[73] P.J. Stephens, F.J. Devlin, C. Chabalowski, Ab initio calculation of vibrational absorption and circular dichroism spectra using density functional force fields, J. Phys. Chem. 98 (1994) 11623–11627, https://doi.org/10.1021/j100096a001.
[74] A.D. McLean, G.S. Chandler, Contracted gaussian basis sets for molecular calculations. I. Second row atoms, Z=11–18, J. Chem. Phys. 72 (1980) 5639–5648, https://doi.org/10.1063/1.438980.
[75] K. Raghavachari, J.S. Binkley, R. Seeger, J.A. Pople, Self-consistent molecular orbital methods. XX. A basis set for correlated wave-functions, J. Chem. Phys. 72 (1980) 650–654, https://doi.org/10.1063/1.438955.
[76] J.-P. Blaudeau, M.P. McGrath, L.A. Curtiss, L. Radom, Extension of Gaussian-2 (G2) theory to molecules containing third-row atoms K and Ca, J. Chem. Phys. 107 (1997) 5016–5021, https://doi.org/10.1063/1.474865.
[77] T. Clark, J. Chandrasekhar, G.W. Spitznagel, P.v.R. Schleyer, Efficient diffuse function-augmented basis sets for anion calculations. III. The 3-21+G basis set for first-row elements, Li–F. J. Comp. Chem. 4 (1983) 294–301, https://doi.org/10.1002/jcc.540040303.
[78] S.F. Boys, F. Bernardi, The calculation of small molecular interactions by the differences of separate total energies. Some procedures with reduced errors, Mol. Phys. 19 (1970) 553–566, https://doi.org/10.1080/00268977000101561.
[79] G. Scherillo, G. Mensitieri, A. Baldanza, V. Loianno, P. Musto, M. Pannico, A. Correa, A. De Nicola, G. Milano, Weak interactions between Poly(ether imide) and carbon dioxide: a multiscale investigation combining experiments, theory, and simulations, Macromolecules 55 (2022) 10773–10787, https://doi.org/10.1021/acs.macromol.2c01382.
[80] L.F. Cameretti, G. Sadowski, Modeling of aqueous amino acid and polypeptide solutions with PC-SAFT, Chem. Eng. Process 47 (2008) 1018–1025, https://doi.org/10.1016/j.cep.2007.02.034.
[81] W. Wagner, A. Pruss, The IAPWS formulation 1995 for the thermodynamic properties of ordinary water substance for general and scientific use, J. Phys. Chem. Ref. Data 31 (2002) 387–535, https://doi.org/10.1063/1.1461829.
[82] B.D. Marshall, C.P. Bokis, Revisiting the treatment of cross-association interactions in oxygenate mixtures with the polar PC-SAFT equation of state, Fluid Phase Equilib. 529 (2021) 112867, https://doi.org/10.1016/j.fluid.2020.112867.
[83] H. Uji-i, S.M. Melnikov, A. Deres, G. Bergamini, F. DeSchryver, A. Herrmann, K. Müllen, J. Enderlein, J. Hofkens, Visualizing spatial and temporal heterogeneity of single molecule rotational diffusion in a glassy polymer by defocused wide-field imaging, Polymer 7 (2006) 2511–2518, https://doi.org/10.1016/j.polymer.2005.11.094.
[84] P. Musto, G. Mensitieri, M. Lavorgna, G. Scarinzi, G. Scherillo, Combining gravimetric and vibrational spectroscopy measurements to quantify first- and second-shell hydration layers in polyimides with different molecular architectures, J. Phys. Chem. B 116 (2012) 1209–1220, https://doi.org/10.1021/jp2056943.